prepared for:

Directorate-General for Public Works and Water Management

Hydraulic Engineering Division

Hydraulic aspects of the dimensioning of geosystems

December 1997

H 3214

WL | delft hydraulics

Hydraulic aspects of the dimensioning of geosystems

M. van der Wal

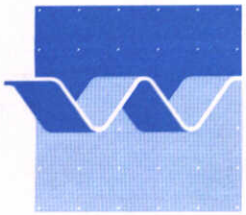

WL | delft hydraulics

WL | delft hydraulics

CLIENT: Directorate-General for Public Works and Water Management
Hydraulic Engineering Division
P.O.Box 5044, 2600 GA Delft

TITLE: Hydraulic aspects of the dimensioning of geosystems

ABSTRACT:

A review of literature related to geosystems has been carried out with respect to calculation methods for the dimensioning of geosystems. The following geosystems have been described in more detail: floating screens, bottom screens and inflatable dams. Floating and bottom screens are made of a synthetic geotextile and kept in position by anchor cables. Inflatable dams are made of a synthetic geomembrane and they are filled with water or with air. Simple calculation methods for the forces and deformations in screens and membranes have been presented. Some field experiences with geosystems have been evaluated.

REFERENCES: Contract no DWW-1269

REV.	ORIGINATOR		DATE	REMARKS	REVIEW		APPROVED BY	
3	M.van der Wal		24-12-97	final report	M.Klein Breteler		W.M.K.Tilmans	

KEYWORDS	CONTENTS		STATUS
geosystems, floating screens, bottom screens, inflatable dams	TEXT PAGES:	69	☐ PRELIMINARY
	TABLES:	13	☐ DRAFT
	FIGURES:	24	☒ FINAL
	APPENDICES:	1	
	PROJECT IDENTIFICATION: H 3214		

Contents

List of symbols

A	cross-sectional area of the screen projected perpendicular to the flow direction (m^2)
A_a	cross section of anchor rope (m^2)
A_c	cross section of upper or lower cable (m^2)
A_e	effective area = $L_e\, d_e$ = projected area of a screen perpendicular to the approach flow (m^2)
A_{fl}	cross-section of that part of a float which is above the water surface (m^2)
a_w	particle orbit in waves (m)
C_c	force coefficient in upper or lower cable (-)
C_D	drag coefficient, time averaged (-)
C_D'	root mean squared value of the fluctuating drag coefficient (-)
$C_{D,wi}$	coefficient for the wind drag force (-)
C_L	lift coefficient (-)
C_L'	root mean squared value of the fluctuating lift coefficient (-)
c	damping
c_a	coefficient (-)
c_b	coefficient for the distribution of the drag force on the screen over the upper and lower cable (-)
c_{up}	coefficient for the wind set-up (emperical) (-)
c_{con}	concentration of sediment (kg/m^3)
c_{cur}	coefficient for the influence of the curvature of the screen on the added mass (-)
c_h	coefficient for horizontal force on screen (-)
c_{shp}	coefficient for the shape of the bankline around the screen (-)
c_v	emperical coefficient for vertical force on screen (-)
c_ω	coefficient for the calculation of added mass (-)
d	elongated depth of a screen loaded by a hydrodynamic pressure (m)
d_e	effective depth of a screen (projected perpendicular to the main flow direction upstream of a screen) (m)
d_o	initial depth of a screen without hydrodynamic load (m)
E_c	elasticity modulus for a cable (N/m^2)
E_s	elasticity modulus or Young's modulus for a screen (N/m^2)
$E(\Phi.k)$	Legendre's form for the elliptic integral of the second kind (-)
f	function
F_b	upward force of a float (N)
F_D	drag force (N)
F_D'	drag force caused by vortex shedding (N)
F_h	horizontal component of T_s in the upper end of a screen per unit width of a screen (N/m')
F_L	lift force (N)
F_t	force perpendicular to the cable as a result of tension in the cable (N)
F_{te}	force on the screen caused by temperature differences (N/m')
$F(\Phi,k)$	Legendre's form for the elliptic integral of the first kind (-)
g	acceleration by gravity (m/s^2)
H	wave height (m)
H_{max}	maximum wave height of the incoming wave for the design of a screen (m)
H_s	significant wave height (m)
h	water depth (m)
k	modulus of elliptic functions (-), wave number (-)
L_a	length of anchor rope (m)
L_o	initial length of screen without hydrodynamic load (m)
L	length of elongated screen loaded by hydrodynamic load (m)

L_e	effective length of a screen (projected perpendicular to the main flow direction upstream of the screen (m)
L_f	fetch length (m)
L_w	wave length (m)
M_o	added mass (kg)
m	mass (kg)
P	pressure force (N)
p_w	wave pressure (N/m^2)
R_a	ratio of the maximum amplitude of a orbital particle movement over the maximum slack of the screen (-)
r_b	radius of a circular float (m)
r_{rf}	wave reflection coefficient (-)
T_s	pulling force in a vertical strip of a screen with the unit width (N/m')
T_c	pulling force in upper or lower cable of a screen (N)
$T_{c,x}$	component in x-direction of T_c (N)
$T_{c,y}$	component in y-direction of T_c (N)
u	flow velocity, often over the effective depth of a screen averaged flow velocity, often the undisturbed flow velocity upstream of a screen (m/s)
u_w	horizontal component of the flow velocity of a water particle in a wave (m/s)
u_{wi}	wind speed (m/s)
x	horizontal axis perpendicular to the main approach direction
y	horizontal axis perpendicular to x-axis
y_l	internal pressure in an inflatable dam (m water column)
z	vertical axis
α	angle (degrees)
β	angle between wind direction and normal to screen (degrees)
δ	sag of cable or screen (m)
ϵ	elongation of a membrane or a cable at failure (-)
η	dimensionless y axis (-)
ξ	dimensionless x axis (-)
ρ, ρ_w	density of water (kg/m^3)
ρ_{air}	density of air (kg/m^3)
ρ_{fl}	density of float (kg/m^3)
ρ_s	density of sediment (kg/m^3)
ρ_{slt}	density of silt (kg/m^3)
σ	hydrodynamic load or hydrodynamic pressure upstream of a straight screen, where the flow is undisturbed by the screen (N/m^2)
σ_a	maximum tension in an anchor rope (N/m^2)
σ_c	hydrodynamic force per unit length of the screen (N/m')
σ_s	hydrodynamic pressure perpendicular on a screen (N/m^2)
Θ	angle between T_s and F_h at edge of screen (degrees)
Ψ	angle of the membrane with the horizontal (degrees)

1 Introduction

The application of geosystems in hydraulic engineering is in full development. However, in many situations no reliable and proven calculation methods are available for the dimensioning of geosystems. In this report literature related to geosystems has been reviewed with respect to the dimensioning of geosystems. All relevant references can be found in chapter 3 (appendix 1). Many different geosystems have been constructed and typical applications have been listed in chapter 2. Floating screens (chapter 4), bottom screens (chapter 5) and inflatable dams (chapter 6) have been described in more detail. Floating and bottom screens are made of a synthetic fabric and they are kept in position by anchor cables. Inflatable dams are made of a synthetic membrane and they are filled with air or water. Simple calculation methods for the forces and deformations in screens and membranes have been presented. Some field experiences with geosystems have been evaluated.

Rijkswaterstaat commissioned Delft Hydraulics to carry out the study by letter dated April 22, 1997 (contract no DWW-1269). The study has been carried out by Mr. M. van der Wal while Mr. H.J. Verheij has been the project manager. Rijkswaterstaat has been represented by Mr. K.W. Pilarczyk and Mr. E. Berendsen.

2 Geosystems

An inventory of different geosystems mentioned in the literature has resulted in many different applications in an hydraulic environment. Some typical examples of these applications are:

- surface screens to prevent transportation of polluted sediments or to function as a wave barrier,
- bottom screens to prevent erosion of the sea bottom or to prevent sedimentation in a harbour basin,
- horizontal screens on the beach to prevent erosion,
- two parallel inflatable tubes of membranes as a floating breakwater
- a system of submerged air balloons also as breakwater,
- siltation cloths to prevent erosion and to stimulate sedimentation,
- geotubes and sausages for bank and beach protection
- inflatable dams for flood protection, for water management in irrigation systems and as a flexible submerged breakwater
- a tethered float breakwater,
- geo-containers and geocells for bank protection,
- vertical bundles of fibers to prevent erosion of sea or river bed
- breakwater made of hoses of synthetic material filled with concrete.

From all these applications floating and bottom screens and inflatable dams have been described in more detail in the following chapters. Several of these applications are only theoretical concepts which have to be developed further before the construction of a prototype structure.

3 Set-up of the report

This study has been directed towards the development of calculation methods which can be used for a preliminary dimensioning of geosystems. The development of a calculation method for floating surface screens has received most attention. This development started with a base case of a floating screen with an upper and a lower cable. Both cables have been connected independantly to several anchor ropes. During the study this base case has been extended, for example with a screen of which only the upper cable is kept in position by anchor ropes and the lower cable functions only as ballast. The aim of the report is a systematic approach in all details. A consequence of the considerable efforts to develop a more or less complete calculation method for floating screens is that other systems (bottom screens and inflatable dams) have recieved less attention in comparison with the description of floating screens.

The development of a calculation method started with a literature review. Important hydraulic parameters have been represented by the same symbol in many articles. However, these symbols are not always selected in a systematic way, for example one symbol for forces, one for pressures and one for tensions. In this report it has been preferred to apply the same symbols as used in the literature and to accept some inconsistancy in the symbols for different hydraulic parameters. A clear description of all symbols is given in the list of symbols to prevent confusion.

Literature has been collected from different libraries. Rijkswaterstaat had collected literature related to geosystems and this literature has been used in this report. In addition literature had been collected from other sources during the preparation of this report. A complete list of references is presented in appendix 1.

4 Floating screens

4.1 Constructional aspects

A floating screen exists of a vertical screen which is kept in position by cables, connected with floats and anchor cables. Many different type of screens have been constructed and two main types are:

- Small screens have often only an upper cable, which has been connected with anchor cables at regular intervals. A lower cable is missing or it is a ballast chain for sufficient weight.
- Big screens have often an upper and a lower cable, both have been connected with anchor cables at regular intervals.

A screen can consist of a series of separated sheets (lamellas) between the connecting points with anchor cables. Other types consist of a continuous sheet. Floats can be a series of spheres or cylinders made of polystyrene, polyurethane or other type of synthetic foam.

Screens can be permeable or impermeable. In general screens are made of synthetic materials such as polyester, polypropylene or other materials, but sometimes natural materials are used as well, for example canvas made of cotton with a rubber coating. If necessary, local reinforcement belts and/or metal reinforcements in the corners have been added to the screen. In general steel cables are used in floating screens, but also nylon cables have been applied. Not all screens are permanent structures, also temporary screens are found.

Floating screens in estuaries and other coastal areas are sometimes exposed to severe wave and flow conditions. Silt Protector (Taiyo Kogyo Corporation, 1994) and Ro-Boom screens (Christensen and Kock, 1997) have been designed for conditions mentioned in Table 4.1. The lower cable of a Ro-Boom screen is a ballast cable which is not connected to anchor ropes. It seems that standard floating screens should be applied only in areas with low flow velocities, less than 0.3 m/s. In that table the maximum wave height is the heigth of a non-breaking wave.

Screen type	*Maximum flow velocity*	*Maximum wave height*	*Maximum water depth*
	(m/s)	(m)	(m)
Silt Protector type B	0.25	1.5	15
RO-BOOM type 2000	0.3	0.9	-

Table 4.1 Extreme design conditions of 2 types of floating screens

Some examples of floating screens have been described by Sawaragi (1989,1992) and Silt Protector (Taiyo Kogyo Corporation), see Figure 4.1. In tidal areas an intermediate float has been applied to allow for a large tidal range and a stable positioning of the screen. In deep water floating screens are sometimes combined with bottom screens, see example in Figure 4.1.

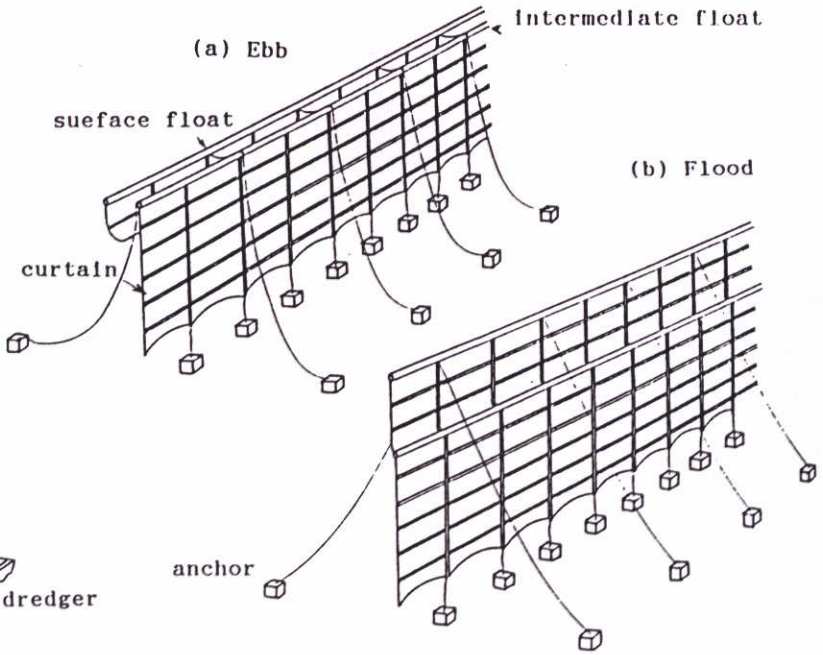

Fig.5 Silt Protector with Intermediate Float for Large Tidal Range

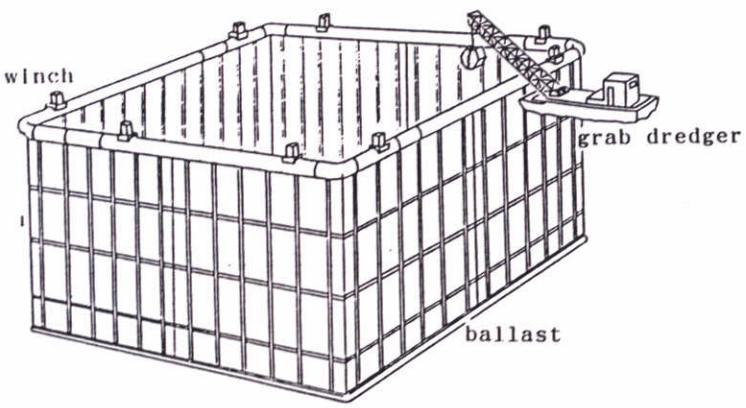

Fig.3 Bucket Type Silt Protector

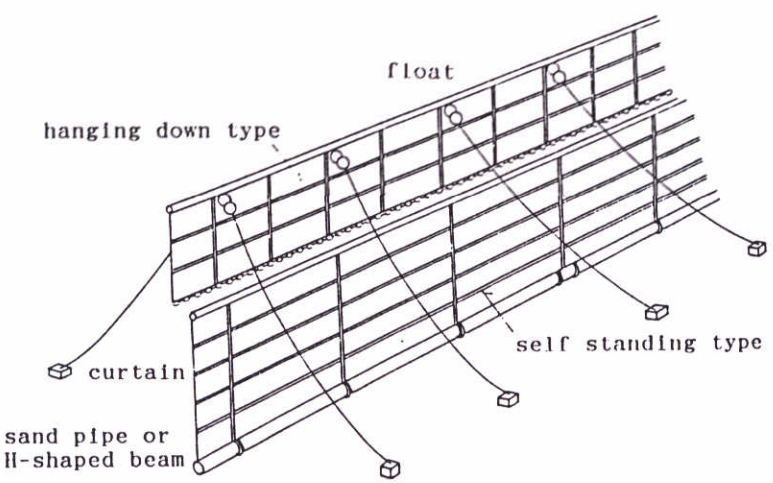

Fig.6 Silt Protector Sheets for Large Depth

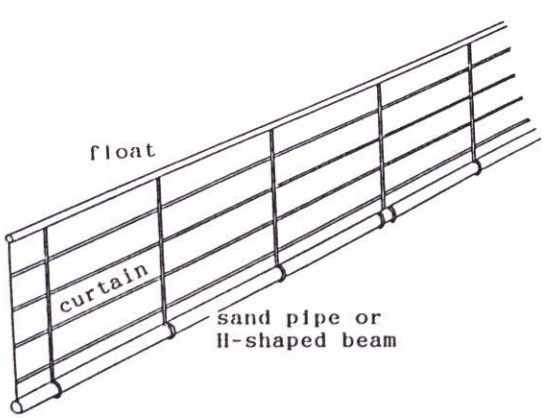

Fig.4 Self Standing Type

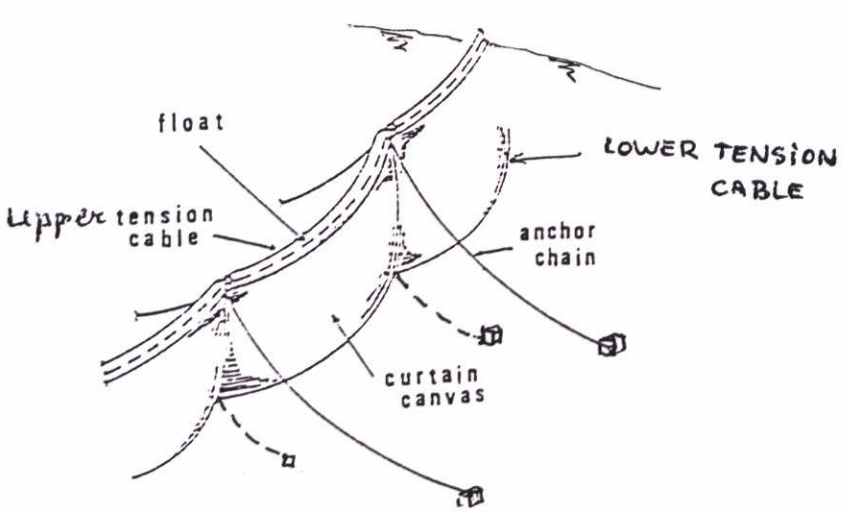

Figure 4.1 Examples of floating screens

4.2 Calculation method

4.2.1 Introduction

A floating screen can be loaded by different hydrodynamic loads. For the dimensioning of a screen a combination of these loads which cause extreme forces in the screen system has to be determined.

Hydrodynamic loads:

1 screen in steady flow (Sections 4.2.2 to 4.2.4)
2 screen loaded by an impulsive force (Section 4.2.5)
3 screen in waves (Section 4.2.6)
4 oscillations and/or vibrations of the screen and oscillating forces (Section 4.2.7)
5 wind force on the floats of a floating screen (Section 4.2.8)
6 forces due to density differences (salinity, oil layer, temperature) and floating debris (Section 4.2.9).

All the forces are transferred to the bed or to the bank by an anchoring system. It is assumed that floating screens will not be used when the water surface has been frozen. Therefore ice loads on floating screens are not considered in this report. It is assumed that each element of a floating screen (screen, cables and floats) has a homogeneous density and elasticity. The permeability of a permeable floating screens varies in most cases in time, for example by vegetation which grows on the screen. In the following a standard floating screen has an impermeable membrane.

The design condition is a combination of the different forces 1 to 5 and the additional forces mentioned under 6 can occur in special situations. Finally, a calculation method has been proposed for the dimensioning of floating screens, Section 4.2.10 and this method has been applied to determine forces and deformation of a screen loaded by waves and steady flow, Section 4.2.11.

4.2.2 Screen in steady flow

A steady flow exerts a drag force on a floating screen:

$$F_D = C_D A_e \frac{1}{2} \rho u^2 \qquad (1)$$

in which

A_e = effective area = $L_e d_e$ = projected area of a screen perpendicular to the approach flow (m^2)
C_D = drag coefficient, time averaged (-)
d_e = effective depth of a screen (m)
L_e = effective length of a screen (m)
u = over the effective depth of the screen averaged approach flow velocity (m/s)
ρ = density of water (kg/m^3)
F_D = drag force, time averaged (N)

If the variation of u over the depth of the screen can not be neglected than the darg force is the sum of the drag force on different slices of the screen or to introduce integration over the depth of the screen.

The hydrodynamic load perpendicular to 1 m^2 of this section:

$$\sigma = \frac{F_D}{A_e} \tag{2}$$

in which σ = hydrodynamic pressure (N/m^2)
This hydrodynamic pressure σ is related to the hydrodynamic load, σ_s, perpendicular to the screen:

$$\sigma_s = \frac{1}{1 + (\frac{df}{dz})^2}\ \sigma \tag{3}$$

in which f(z) describes the shape of the screen as a function of z on the vertical axis. This formula is based on the projection of 1 m^2 in the approach flow on a screen.

The shape of the screen follows from the assumption that the screen transfers only forces in its plane. It is assumed that no water flows along the screen and therefore the friction force between water and screen can be neglected. Force equilibrium on a section of a screen results in (see Figure 4.2):

$$\sigma_s \sqrt{1 + (\frac{df}{dz})^2} - T_s \frac{d^2f}{dz^2} = 0 \tag{4}$$

in which T_s = pulling force in the membrane of the screen (N/m'). The vertical z axis has its origin in the middle of a screen section. In the horizontal plane the y-axis is perpendicular to the x-axis.

The shape of the screen is described by a cosine-hyperbole, which satisfies the differential equation, formula (4):

$$f(z) = \frac{T_s}{\sigma_s} [\cosh(\frac{\sigma_s z}{T_s}) - 1] \tag{5}$$

If the deformation of a screen is small than this cosine-hyperbole can be approximated by a circle, see formula (6), as proposed by Sawaragi, Aoki and Liu, (1992, formula 5 on page 344). The reasons for this approximation are not explained in their article.

The tension T_s (N/m') in the screen causes an elongation of the screen section. In general

$$(y - \frac{T_s}{\sigma_s})^2 + z^2 = (\frac{T_s}{\sigma_s})^2 \tag{6}$$

this elongation follows Hooke's law:

$$\frac{T_s}{A_S} = E_s \cdot \frac{d - d_o}{d_o} \tag{7}$$

in which

A_s	=	cross-section of the screen (thickness * unit length) (m^2)
E_s	=	Young's modulus or elasticity modulus (N/m^2)
d	=	$d_o + \delta d$, depth of the elongated screen (m)
d_o	=	initial depth of the screen without forces acting on it (m)

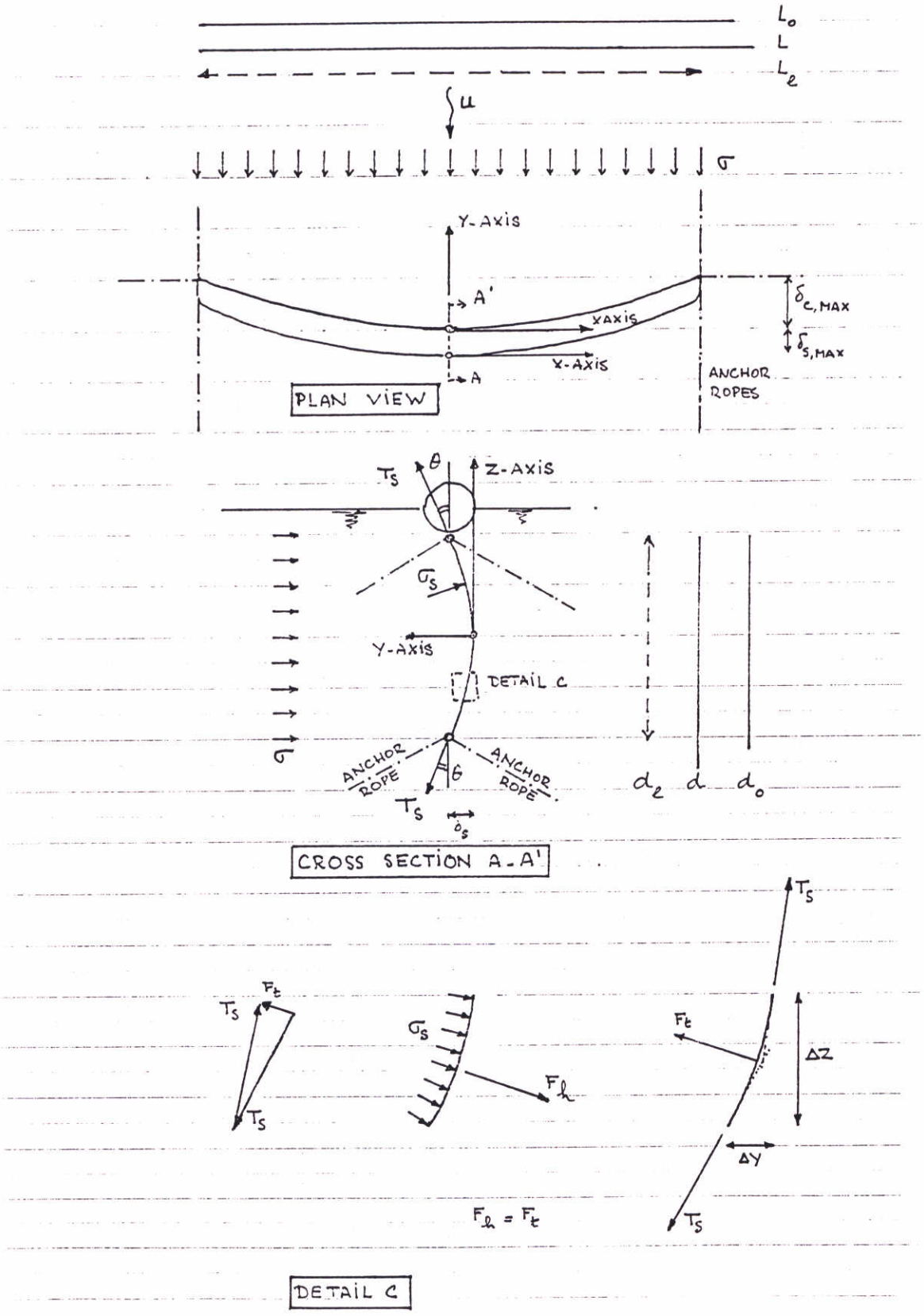

Figure 4.2 Force equilibrium in screen section

The effective depth of the screen (see Figure 4.3) is determined by a line integral:

$$d = \int_{-\frac{1}{2}d_e}^{\frac{1}{2}d_e} \sqrt{1 + (\frac{df}{dz})^2}\, dz = \frac{2\ T_s}{\sigma_s} \sinh(\frac{\sigma_s\ d_e}{2\ T_s}) \qquad (8)$$

in which d_e = effective depth of a screen, projected perpendicular to the main approach flow direction (m)

The boundary condition is that in both ends the horizontal component of T_s makes an equilibrium with the hydrodynamic load (Sawaragi, Aoki and Liu, 1992, formula 7 on page 344):

$$F_h = \frac{1}{2}\sigma\ d_e \qquad (9)$$

in which F_h = horizontal component of T_s in the upper end of a screen (N/m'). This formula assumes that the hydrodynamic load is uniform over the screen and that load is transferred symmetrical to the upper and lower ends of a screen. In case of a vertical velocity profile with a well developed boundary layer flow this is a strong schematization. In general the upper edge (connected with the upper cable) will take more load than the lower edge (connected with the lower cable). A more general form of formula (9):

$$F_{h,u} = (1 - c_b)\ \sigma\ d_e$$
$$F_{h,l} = c_b\ \sigma\ d_e \qquad (10)$$

in which

c_b	=	coefficient (-) and in general $0 < c_b < 1$.
$F_{h,u}$	=	horizontal force in upper edge of screen (N/m')
$F_{h,l}$	=	horizontal force in lower edge of screen (N/m')

This boundary condition results in the following formulas:

$$\sin\Theta = \frac{F_h}{T_s} \qquad (11)$$

in which Θ is the angle between T_s and F_h in the upper edge of a screen.

$$\tan\Theta = \frac{df(0.5d_e)}{dz} = \sinh\frac{\sigma_s\ d_e}{2\ T_s} \qquad (12)$$

$$T_s = F_h \frac{\sqrt{1 + \tan^2\Theta}}{\tan\Theta} \qquad (13)$$

Combination of (7) and (8) results in:

$$\sinh(\frac{\sigma_s\ d_e}{2\ T_s}) = \frac{d_o\ \sigma_s}{2\ T_s} + \frac{(d-d_o)\ \sigma_s}{2\ T_s} = \frac{d_o\ \sigma_s}{2\ T_s}(1 + \frac{T_s}{A_s\ E_s}) \qquad (14)$$

This formula shows some similarity with Sawaragi, Aoki and Liu (1992, formula 6 on page 344).

The proposed calculation method for a screen starts with the assumption of a value of Θ and to use d_o as a first estimate of d_e. After calculating σ by (2) and (1) T_s is estimated by:

$$T_s = (1 - c_b)\, \sigma\, d_o \frac{1}{\sin\theta} \tag{15}$$

Calculate σ_s:

$$\sigma_s = \frac{2\, T_s}{d_o \left(1 + \frac{T_s}{A_s\, E_s}\right)} \tan\theta \tag{16}$$

Calculate d_e:

$$\sinh\left(\frac{\sigma_s\, d_e}{2\, T_s}\right) - \tan\theta = 0 \tag{17}$$

Repeat the calculation of T_s and σ_s with d_o replaced by d_e.
Calculate d:

$$d = d_o + \frac{T_s\, d_o}{A_s\, E_s} \tag{18}$$

For different synthetic materials the elongation at failure is presented in Table 4.2. If a minimum safety factor of 2 is selected, than the following rule is proposed for a good design of the thickness of the screen:

$$1 + (\epsilon - 1)/10 < \frac{d - d_o}{d_o} < 1 + (\epsilon - 1)/2 \tag{19}$$

in which ϵ = elongation of the membrane at failure.
If the elongation in a design calculation is very small than the membrane is too thick and in case the elongation is too large than the thickness of the membrane should be increased.
Calculate the maximum sag of the screen:

$$\delta_{s,max} = \frac{T_s}{\sigma_s}\left[\cosh\frac{\sigma_s\, d_e}{2\, T_s} - 1\right] \tag{20}$$

Repeat this calculation for different values of Θ and select from the calculated results a design value of Θ. For an unequal distribution of the maximum force over the length of the screen a safety factor, for example 2, for the steady flow is recommended.

Synthetic material	*elongation at failure, ϵ*	*minimum elongation*	*maximum elongation*
	%	%	%
PET	13	1.3	6.5
Polypropylene	20	2	10
Polyamide	20	2	10
Aramide	3.7	0.4	1.85
Dyneema SK60	3.5 to 5	0.35	2.5

Table 4.2 The proposed maximum and minimum elongation and elongation at failure of synthetic materials (TNO, 1997).

4.2.3 Cables in steady flow

The pulling force in a screen T_s (N/m' width of the screen) can be resolved in a vertical component F_v and a horizontal component F_h. This vertical component together with the weight of the cables and the vertical component of the force in the anchor cables make equilibrium with the floating force of the floats. This horizontal component is transferred by the cables to the anchor ropes. In general the upper cable and the lower cable are connected with separate anchor ropes. In case of a small screen only the upper cable of some smaller screens is connected with anchor ropes and the lower cable functions as ballast to keep the screen in a more vertical position.

The approach flow exerts a drag force on a projected screen normal to the flow direction. The total drag force F_D according to formula (1) is transferred partly to the upper cable (index u) and partly to the lower cable (index l):

$$\sigma_u = C_D \frac{1}{2} \rho u^2 (1 - c_b) d_e = \frac{F_D}{A_e} (1 - c_b) d_e \qquad (21)$$

and

$$\sigma_l = C_D \frac{1}{2} \rho u^2 c_b d_e \qquad (22)$$

in which σ_u and σ_l (N/m'perpendicular to the main flow direction) are parallel to the main flow direction in the approach flow. In these formulas the following definitions have been used:

$$A_e = L_e d_e \qquad (23)$$

in which L_e = the effective length of a screen (m)
In the following the indices u and l (upper and lower respectively) have been omitted, because these formulas can be applied to both.

The load perpendicular to the cable of the screen, see scheme in Figures 4.2 and 4.3:

$$F_h = \sigma_c \frac{1}{1 + [\frac{df}{dx}]^2} \qquad (24)$$

in which
f(x)= function describing the shape of the cable. In a horizontal plane the x-axis is perpendicular to the main direction in the approach flow. The y-axis is parallel to the main direction in the approach flow.
F_h is the horizontal component of T_s. The calculation of T_s has been presented in the previous section.
This load on the screen makes an equilibrium with the force due to the tension in the cable, see Figures 4.2 and 4.3 (Milgram, 1971 and Sawaragi et al 1989):

$$F_t = T_c \frac{d^2f}{dx^2} \frac{1}{(1 + [\frac{df}{dx}]^2)^{1.5}} \qquad (25)$$

in which
T_c = tension force in cable (N)
F_t = force perpendicular to T_c (N).

Equilibrium of these two forces (F_t en F_h) results in a differential equation, which solution f(x) describes the shape of the screen in a horizontal plane:

$$\sigma_c \sqrt{1 + [\frac{df}{dx}]^2} - T_c \frac{d^2f}{dx^2} = 0 \qquad (26)$$

This formula which describes the deformation of a cable is comparable with (4) for the screen.
If the origin of the x,y axis is selected that f(0) = df(0)/dx = 0, see Figure 4.3, than the solution is:

$$f(x) = \frac{T_c}{\sigma_c} [\cosh(\frac{\sigma_c x}{T_c}) - 1] \qquad (27)$$

This formula for a cable is comparable with (5) for a screen.
In case the screen is perpendicular to the main flow direction (α = 0 degrees) the origin of the x,y axis is in the middle of the cable. It is mentioned that this origin does not coincide with the origin of the z-axis defined for the calculation of d and T_s in the previous section. The origin of the z-axis is in the middle of a vertical section of a screen.

The tension T_c in the cables follows from a line integral to calculate the length L of the screen, if L, σ_c, x_1 and x_2, ordinates of begin and end of a cable, are given:

$$L = \int_{x_1}^{x_2} \sqrt{1 + (\frac{df}{dx})^2}\, dx = \frac{T_c}{\sigma_c} [\sinh\frac{\sigma_c x_1}{T_c} - \sinh\frac{\sigma_c x_2}{T_c}] \qquad (28)$$

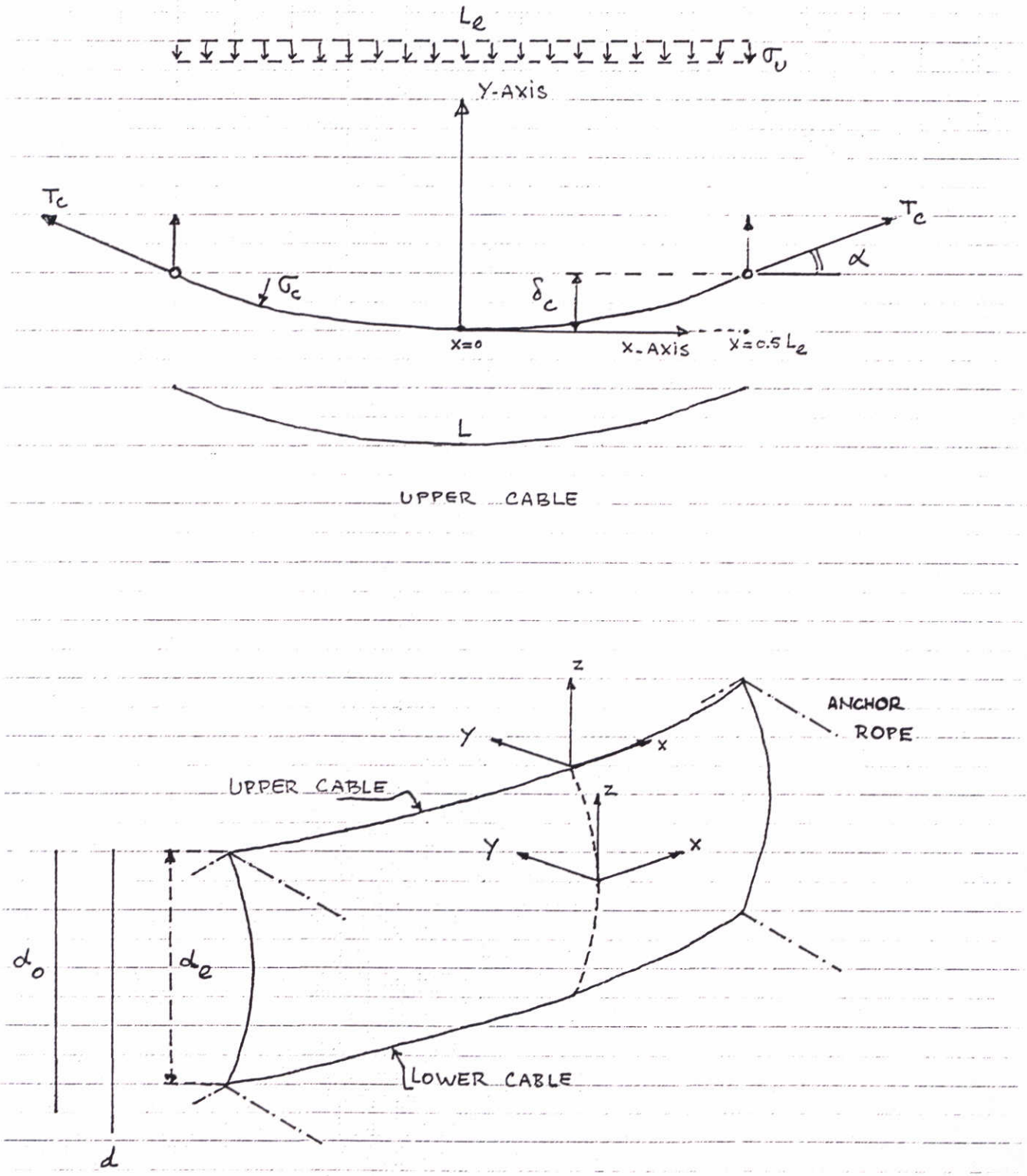

Figure 4.3 Definition sketch of screen paramaters

A simple solution is obtained for the case the screen is symmetrical about the y axis. This means $x_1 = 0.5\ L_e$ = x-ordinate of end of a cable and $x_2 = -0.5\ L_e$ = x-ordinate of begin of a cable:

$$L = \frac{2T_c}{\sigma_c} \sinh\frac{\sigma_c L_e}{2\ T_c} \qquad (29)$$

If the length of the screen L, the hydrodynamic load σ_c and L_e are given than tension T_c can be calculated from (29).

If the elasticity modulus of the steel cables is assumed to be much higher than the elasticity modulus of the screen geotextile than Hooke's law applied on the cables governs the cable forces (Sawaragi et al, 1989):

$$\frac{T_c}{A_c} = E_c \frac{L-L_o}{L_o} \qquad (30)$$

in which

A_c = cross section of cable (m^2)
E_c = elasticity modulus of a cable (N/m^2)
L_o = initial length of a cable without load (m)
L = $L_o + \Delta L$, length of a cable with load (m)

A cable has a constant cross-section over its length.

The maximum displacement or sag of the cable is δ_c and it follows from substitution of x = $0.5\ L_e$ in (27):

$$\delta_c = \frac{T_c}{\sigma_c} (\cosh\frac{\sigma_c\ 0.5\ L_e}{T_c} - 1) \qquad (31)$$

The above formulas for the calculation of T_c, L and δ_c are valid for the upper cable and also for the lower cable. In this calculation it is assumed that the pretension in the cables is zero, this means that if the flow velocity is zero the forces in the screen and cables are also zero (neglecting the forces because of the weight of the screen and cables). If necessary a pretension and weight forces of screen and cables can be included in the presented calculation method.

The tension force in the cable and maximum displacement can be presented in a dimensionless form, see for examples Figure 4.4 (Sawaragi etal 1989 and Milgram, 1971).

According to the theory presented above the shape of the screen can be described with a cosh-function. Silt Protector (Taiyo Kogyo Corporation, 1994) had proposed a simple parabolic-function to approximate this cosh-function. The formula for the calculation of the cable tension can be replaced by:

$$T_c = \frac{\sigma_c\ 0.5\ L_e}{2\ \delta_c} \sqrt{(0.5\ L_e)^2 + (2\delta_c)^2} \qquad (32)$$

in which

L_e = effective length of the screen between the anchor points (m)
δ_c = deformation of the center of the cable (m)
σ_c = horizontal component of the hydrodynamic load on the cable (kg/m')

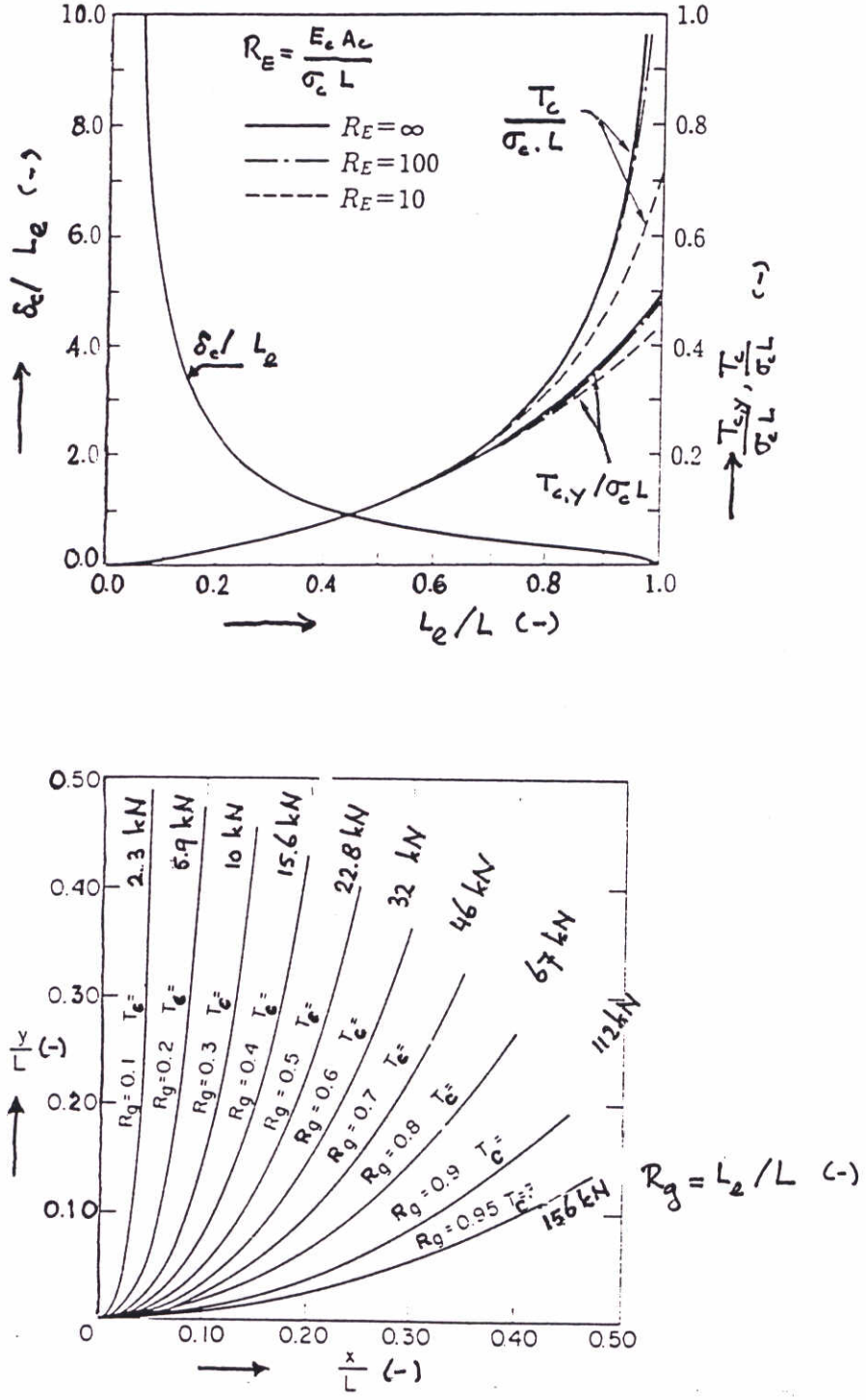

An example of the shape of an upper cable in a steady flow. The shape of the left half of the cable as function of different tensions in the cable and a constant load σ_u = 6440 N/m'.

Figure 4.4 Dimensionless graphs according to Sawaragi and Milgram

For the design of a screen Silt Protector suggests to select a certain angle of 21.8 degrees between the upper cable and the x-axis at connecting points with an anchor rope. In a formula:

$$tg\ 21.8 = 0.4 = \sinh\left(\frac{\sigma_c L_e}{2 T_c}\right) \qquad (33)$$

Results of physical model investigations

The hydrodynamic drag force on a screen induced by a steady flow can be calculated by (1):

$$F_D = C_D \frac{1}{2} \rho u^2 A_e \qquad (34)$$

in which:

u	=	undisturbed upstream flow velocity (often depth averaged) (m/s)
A	=	effective cross-sectional area of the screen projected perpendicular to the flow direction (m^2)
C_D	=	drag coefficient (-)
F_D	=	drag force (N)
ρ	=	specific density of water (kg/m^3).

If a screen can be compared with a flat plate perpendicular to the flow than C_D = 1.5 to 2 (time averaged value) and the fluctuating part $C_D' = 0.15$ (= root mean square of the time dependent value - time averaged value) because of vortex shedding of the flow (CIRIA, UR8, 1977). The value of C_D depends on the shape of the screen structure.

In addition to a drag force the flow induces a smaller lift force perpendicular to the flow direction. This lift force is described in Section 4.2.5 on oscillating forces.

The tension force in the upper and lower steel cables of a canvas screen has been measured in a physical model investigation in a flume (Sawaragi etal, 1989). The tension force T_c:

$$T_c = C_c \frac{1}{2} \rho u^2 A \qquad (35)$$

in which $A = L_e d_o$ = projected width multiplied by the not-projected depth of screen, according to Sawaragi, who conducted tests with a screen in a flume with a constant width. It is recommended to consider a consistent definition based on the projected area (projected depth multiplied by projected width). This coefficient C_c is not the same coefficient as C_D and the relationship between these coefficients is:

$$\frac{C_D}{C_c} \frac{L}{L_e} \frac{d_e}{d_o} \frac{(1 - c_b)}{2} = \sinh\left[\frac{C_D}{C_c} \frac{(1 - c_b)}{2} \frac{d_e}{d_o}\right] \qquad (36)$$

In general the difference between C_c and C_D is probably not negligible, but for a first approximation it is assumed that $C_c = C_D$.

The force coefficient in the upper cable, $C_{c,u}$, follows from an emperical formula (37) based on the measurements in that physical model investigation, see Figure 4.5:

$$C_{c,u} = c_a + 12.3\,(\frac{d}{h} - 0.27)^2 \qquad (37)$$

in which:

c_a	=	coefficent (-) which varies between 2 and 3
d	=	depth of screen (m)
h	=	water depth (m).

In the physical model investigation the force coefficient in the lower cable is smaller than the force coefficient in the upper cable, on average:

$$C_{c,l} = c_b\, C_{c,u} \qquad (38)$$

The coefficient c_b varies between 0.3 to 0.5 and it depends on the flow velocity profile in the approach flow. The forces in the cables are not dependent on the Froude number in the range Fr = 0.05 to 0.3, see Figure 4.6. It might be that the forces in the cables depend on the ratio of the elasticity modulus for steel and for canvas: $2.1*10^{11}$ N/m^2 and $1*10^8$ N/m^2 respectively (Sawaragi, 1992). In this model investigation the discharge could flow only under the screen. In the field this applies to the mid sections of very long screens. In case of a short screen a part of the discharge will be diverted left or right of the screen and the drag force coefficients $C_{c,u}$ and $C_{c,l}$ will depend less on d/h.

This empirical formula for C_c as function of d/h can be compared with drag force coefficient measured in model tests on a caisson with different clearances, see Figure 4.7 (Delft Hydraulics, 1969 and Huis in 't Veld et al, 1987). This confirms the tendency that C_c increases as d/h increases.

The coefficient C_D also depends on the direction of the approach flow. In general an empirical expression is proposed: $C_D.\cos^2 \alpha$ in which α is angle of the approach flow with y-axis. However, CIRIA (1977) mentioned that $C_D.\cos \alpha$ fits better with the measurements. For example, this can be seen in Figure 4.8 where C_D on a caisson as function of α is shown for a submerged body and a floating caisson (Nakamura and Mizota, 1971). These results show that the assumption that C_D for a floating body is the same as for a submerged body is not generally valid. Sawaragi (1989) used this empirical relationship for the force on a screen, depending on the angle of a screen with the flow. It is recommended to use C_D cos α for a floating screen if $\alpha < 45$ degrees.

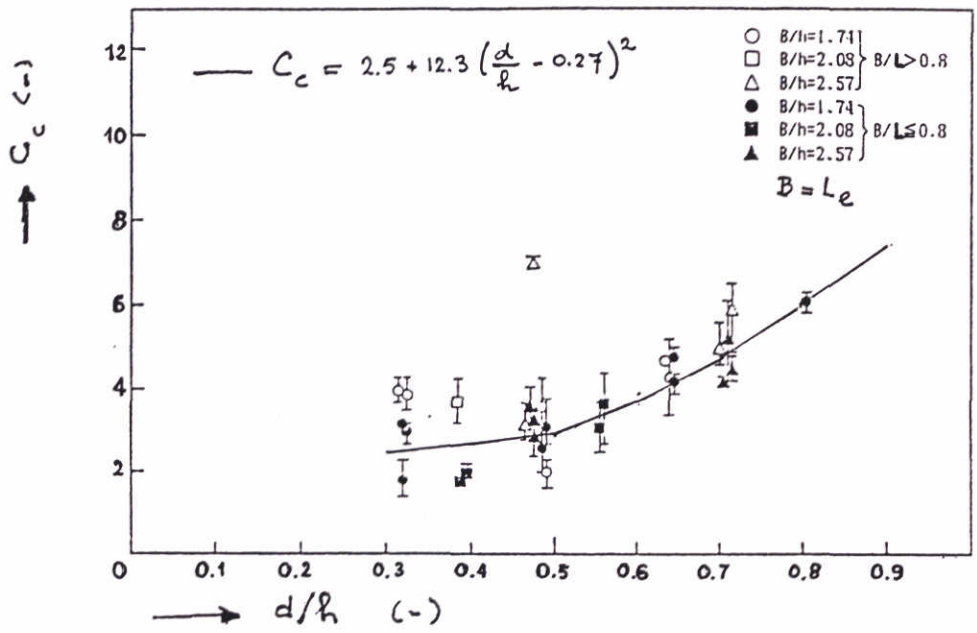

Figure 4.5 Results of model investigation (Swaragi)

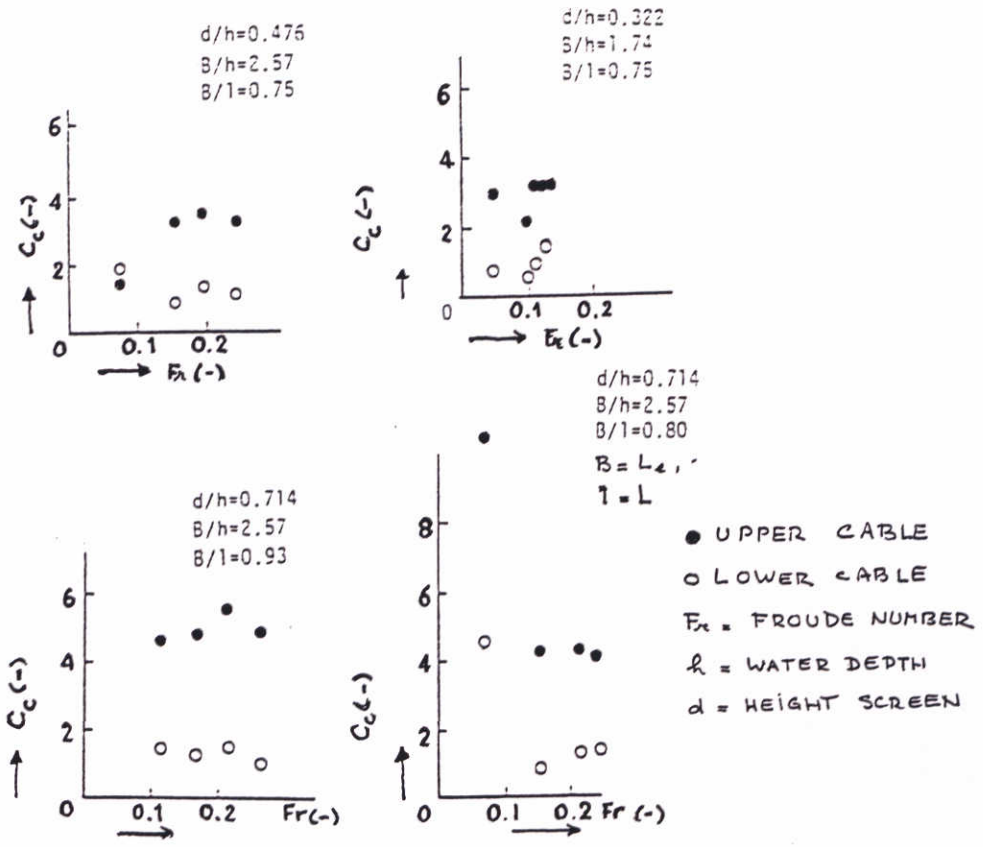

Figure 4.6 Coefficients of the maximum tension measured in model tests

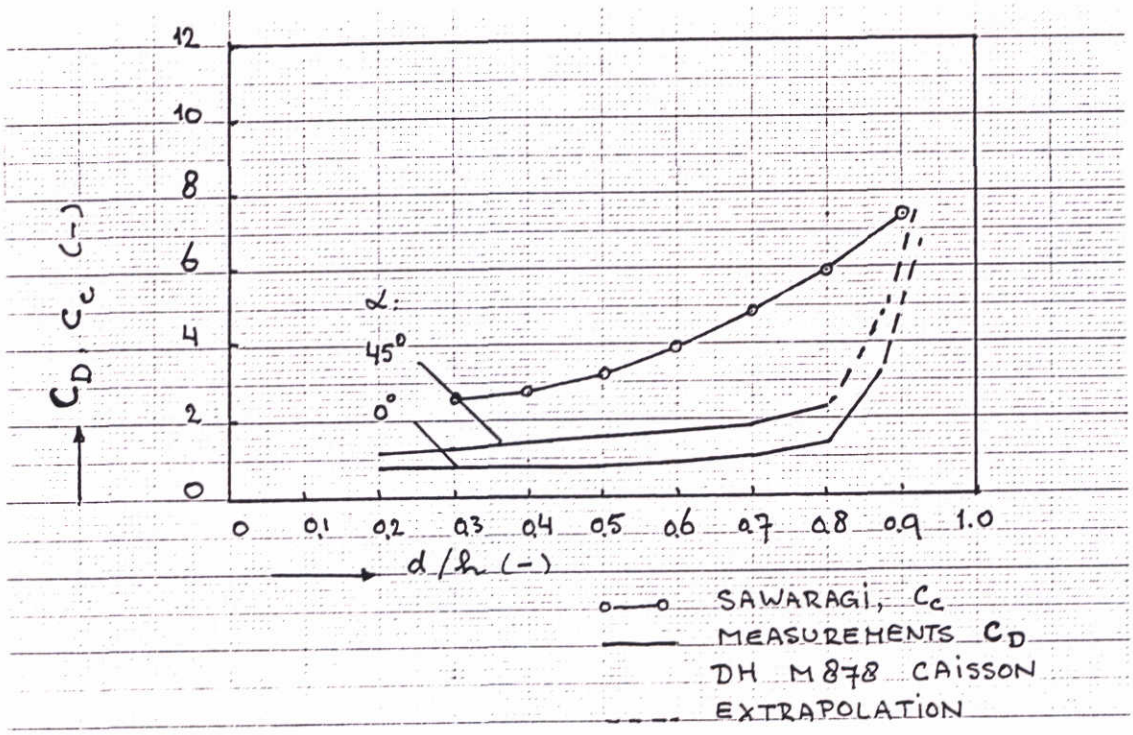

Figure 4.7 C_D as function of the clearance of a caisson

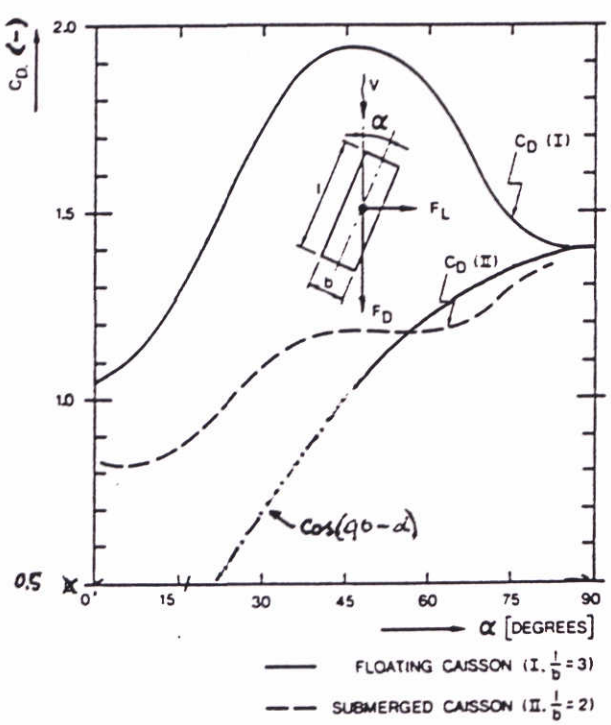

Figure 4.8 Drag coefficient of a floating caisson and a submerged body as a function of the direction of the approach flow

4.2.4 Anchor forces

The cable force T_c in an anchored screen system is transferred to the ropes of the anchors. The cable force T_c can be resolved in $T_{c,x}$ and $T_{c,y}$. $T_{c,x}$ is transferred to an side anchor perpendicular to the flow and $T_{c,y}$ is transferred to an anchor parallel to the flow direction. A minimum of eight anchors are needed for anchoring of a screen in a steady flow (four for the upper cable and four for the lower cable). More anchors are needed if the interval along the screen where anchor ropes are connected has to be reduced, for example, because:

- the forces are too high for the available anchors or standard ropes or
- the deformation of the screen is too large.

If these intervals are regular than the mid anchor ropes are loaded by 2 $T_{c,y}$ annd the end anchors by $T_{c,y}$.

On the other side if the dynamic response of the screen to wave loading induces too high forces in the screen, cables and anchors, than it might be considered to reduce this interval to reduce the forces and to increase the freedom for dynamic deformations of the screen. This depends on the resonance frequency of a screen loaded by waves. If the frequency of the waves is close to the resonance frequency large excitations and large forces can be induced in the screen system (= screen and its anchoring). This phenomena should be investigated for a specific screen in a physical model investigation. In general it should be avoided that the resonance frequency of a screen system is close to the frequencies of waves with the largest amplitudes.

Silt Protector recommends to design anchor ropes or cables with an angle of 30 degrees with the horizontal at the connecting point with the upper or lower cables of the screen. The anchor force is 2.3 $T_{c,y}$ for mid anchors, 1.15 $T_{c,y}$ for end anchors and 1.15 $T_{c,x}$ for side anchors.

The required minimum cross-section of an end anchor rope according to Silt Protector:

$$A_a \geq \frac{1.15\ T_{c,y}}{\sigma_a} \qquad (39)$$

in which

A_a = minimum required cross sectional area of the anchor rope (m^2)

σ_a = maximum tension in a rope (N/m^2). It is recommended to include a safety factor of at least 3.

A minimum length, $L_{a,u}$, of the anchor ropes connected with the upper cable can be estimated by (40). This length is the same for mid, end and side anchors. However, Silt Protector considers half of this length sufficient. It is recommended to use ample length for the anchor ropes. This length might depend on the type of subsoil.

$$L_{a,u} \geq 2\ (h_{max} + 0.5\ H_{max}) / \sin 30^o \qquad (40)$$

in which

H_{max} = maximum design wave height (m)

h_{max} = maximum design water depth (m)

A minimum length $L_{a,l}$ for the anchor cables connected with the lower cable is:

$$L_{a,l} \geq 2\ (h_{max} - d_e) / \sin 30^o \qquad (41)$$

For temporary screens a low cost anchor is recommended, for example concrete blocks or a gabion filled with stones. This type of anchors can hold 2 to 3 times their weight. For permanent screens many different types of (ship) anchors are available.

4.2.5 Impulsive force due to unsteady flow

An impulsive force due to sudden tightening of the screen in a steady current has been studied by Sawaragi et al (1992) in a physical model. The results of these tests show that C_c and C_D can increase 50 to 100 % and that the coefficients $C_{c,u}$ for the upper cable and $C_{c,l}$ the lower cable have the same value for the impulsive force, see Figure 4.9. Probably these results depend on the investigated screen, especially the elasticity of cables and membrane.

Impulsive forces can be caused by a single phenomena or by wave loading. It is assumed that a single phenomena can be schematized as a single wave which amplitude of the orbital particle movement is calculated by formulas (49), (50) or (51). In general impulsive forces are important for the dimensioning of a screen, especially if $u_{flow} < u_{orbital}$.

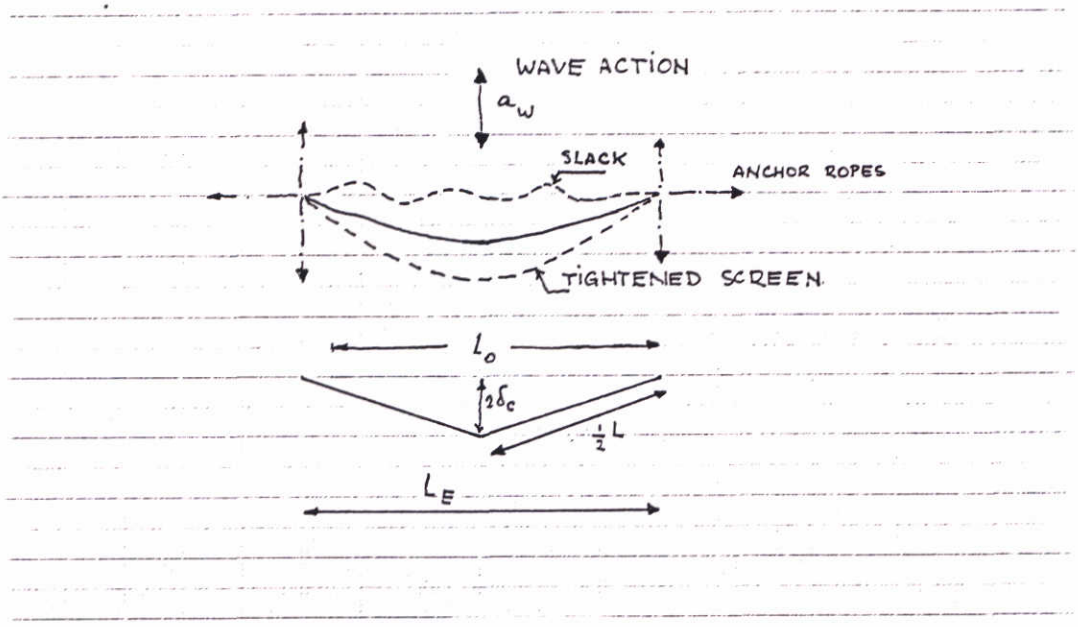

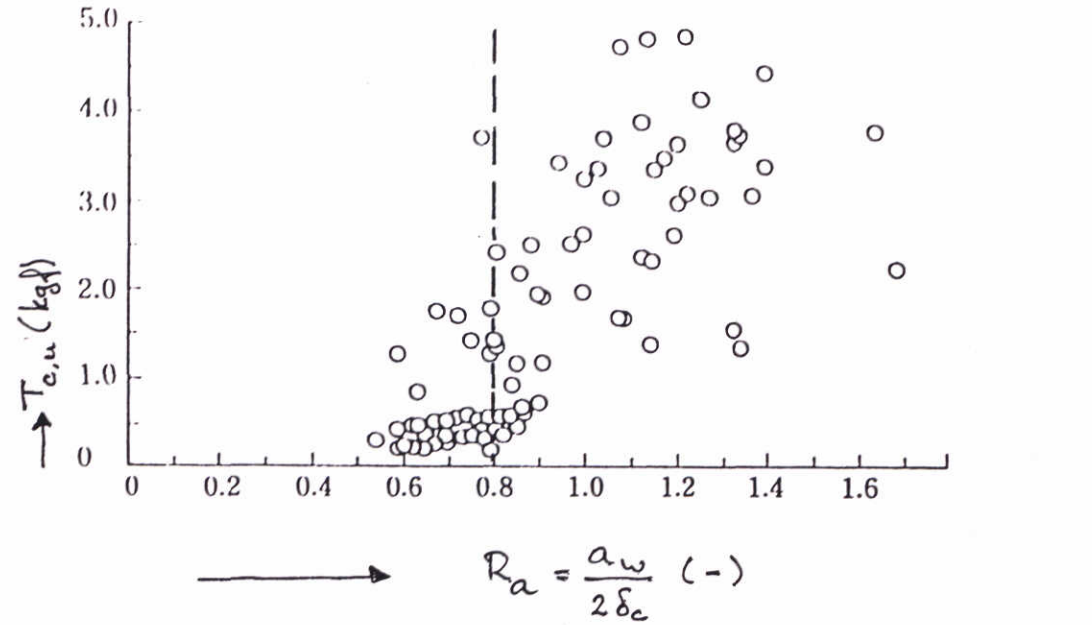

Figure 4.9 Screen response to wave action

In a schematized approach the impulsive force is concentrated in the middle of a screen and a criterium for a slack or tightened screen is R_a, see Figure 4.10:

$$R_a = \frac{a_w}{0.5\sqrt{L^2 - L_e^2}} \qquad (42)$$

in which

a_w = (maximum) amplitude of the orbital particle movement in a wave (m)
L_e = effective length of the screen (m)
L = length of a screen under hydraulic load due to steady flow (m). If no steady flow and only waves, than L should be replaced by L_o.

$R_a > 1$ than the screen is tightened and high forces are induced in the screen. In this situation the drag coefficient can increase 50 to 100% according to the model investigation. $R_a < 1$ than the screen is slack and the screen can follow the water movement without significant increase of the forces in the screen. The material properties, fatigue and aging can be decisive for the design of the screen.

Results of model test (Sawagari, 1992) showed that if $R_a < 0.8$ the forces in the screen and cables are almost zero and if $R_a > 0.8$ these forces increase significantly, see Figure 4.10.

Forces on the screen, cables and anchor ropes due to an impulsive load increase because the water around the screen starts to move with the screen and the mass of the screen system seems to be increased with an added mass M_o.

$$F = (m + M_o)\frac{du}{dt} \qquad (43)$$

in which

F = force (N)
m = mass of a screen system (kg)
M_o = added mass (kg)
du/dt = acceleration (m/s^2)

Assume that the added mass of a screen can be calculated with the same formula as the formula for the added mass of a vertical plate (Sawaragi, 1992):

$$M_o = c_\omega \, c_{cur} \frac{1}{2} \rho \, d_e^2 \qquad (44)$$

in which

c_ω = coefficient for the vibration frequency of the screen (-)
c_{cur} = coefficient for the curvature of the screen compared with a plate which curvature is zero (-)
M_o = added mass per unit length of screen (kg/m')
d_e = the effective depth of the screen (m).
ω = vibration frequency of the screen (s^{-1})

The vertical curvature of a screen is characterized by the ratio d_o/d_e. In case of an impulsive force ω has to be estimated by a strong schematization of the impulsive force.

$\omega/\sqrt{(g/d)}$	c_ω
> 6	1
1.5 ... 6	0.4 ... 1
0.5 ...1.5	3

d_o/d_e	c_{cur}
1.0 ... 1.1	1
1.1 ... 1.3	0.8
>1.3	0.7

Tables 4.3 a and b Recommended values of c_ω and c_{cur} for $d_o/h = 0.5$.

Assume that the elasticity modulus of the canvas screen is higher than the elasticity modulus of the cables; it means that the stiffness of the screen is relatively high. The screen moves with steady flow until $t = 0$ when the screen is tightened up. During Δt after $t = 0$ the cable expands due to the hydrodynamic force. Estimate Δt and δ_c of the middle point of the cable. The acceleration of the middle point of the cable follows from (Sawaragi):

$$\frac{du_c}{dt} = \frac{2(\delta_c - u_0 \Delta t)}{\Delta t^2} \qquad (45)$$

And the hydrodynamic force induced by this acceleration is:

$$\sigma_{c,i} = -\frac{1}{2} M_o \frac{du_c}{dt} \qquad (46)$$

in which M_o = added mass of the screen defined by formula (44), its own mass can be neglected compared to the added mass of water.
The tension force in a cable and the maximum displacement of a cable can be calculated by the formules treated under steady flow, respectively (32) and (31). In an iterative process this maximum displacement should be equal to the estimated δ_c.

A similar calculation method can be applied for the screen if the elasticity modulus of the screen is lower than the elasticity modulus of the cables. In the presented calculation method the parameters of the cables should be replaced by the screen. The results of the physical model investigation reported by Sawaragi showed fair similarity between measured and calculated cable forces.

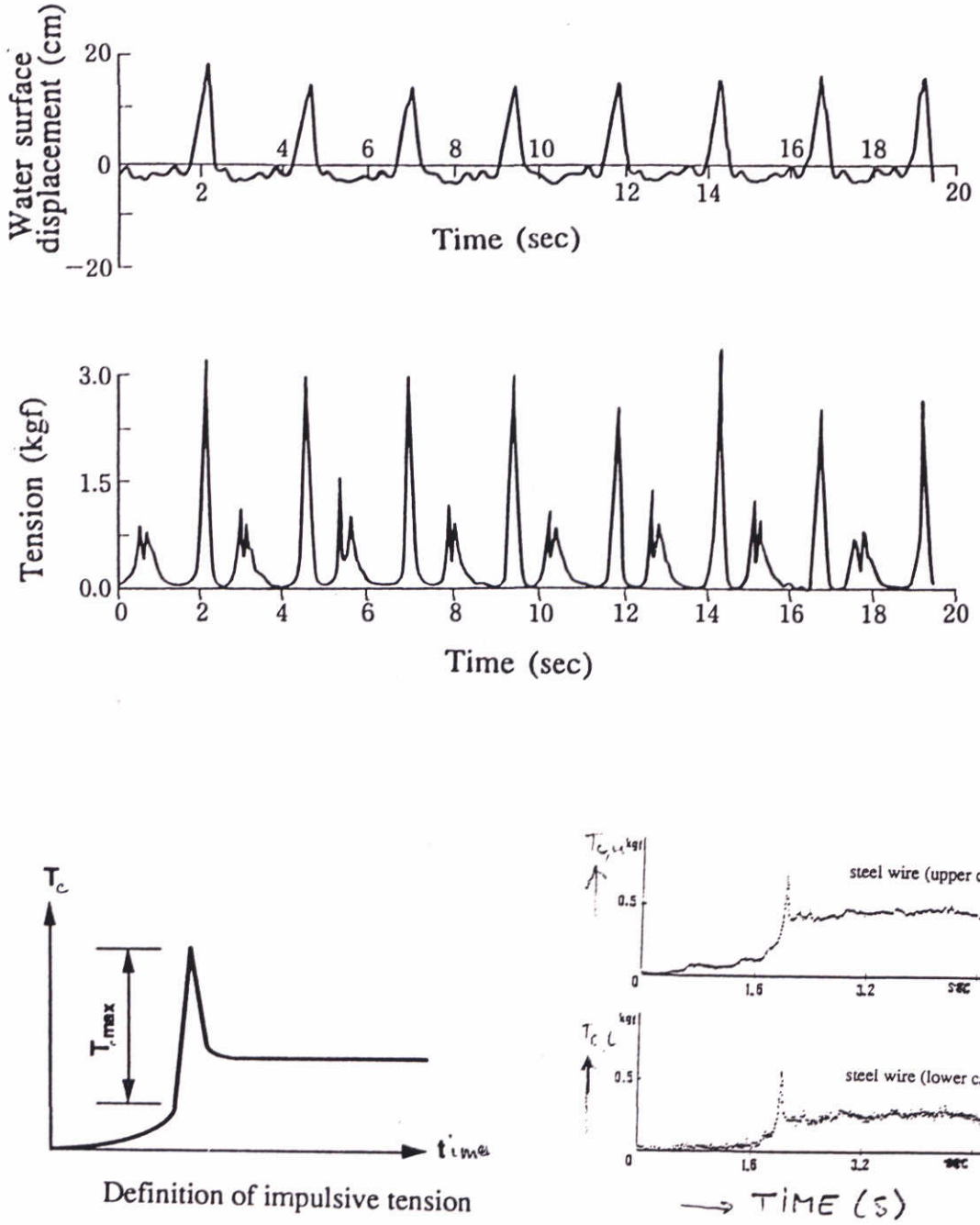

Figure 4.10 Example of impulsive force measured in model investigation (Sawaragi)

4.2.6 Screen in waves

Linear wave theory
Some wave characteristics are derived from the linear wave theory. Linear wave theory is so termed following a linearisation of the boundary condition at the air-water interface, y = 0. The free water surface profile at time t, $\eta(t)$:

$$\eta(t) = \frac{H}{2} \cdot \cos(2\pi \left(\frac{x}{L_w} - \frac{t}{T}\right)) \qquad (47)$$

in which:
H = wave height (m)
L_w = wave length (m)
T = wave period (s)
x = axis in wave direction (m)
t = time (s)
The x-axis is the horizontal axis, the z-axis is measured positive upwards from the mean-water level. The horizontal flow velocities and the horizontal amplitude of the water particles orbit determine the forces and the movements of the floating screen. These parameters can be calculated with the following expressions:

Horizontal flow velocity u_w of a water particle:

$$u_w = \frac{\pi H}{T} \left(\frac{\cosh 2\pi(z + h)/L_w}{\sinh 2\pi\, h/L_w}\right) \cos\left(2\pi \left(\frac{x}{L_w} - \frac{t}{T}\right)\right) \qquad (48)$$

in which
h = water depth (m)
z = vertical axis with its origin at the still water level (m).

Maximum horizontal particle amplitude a_w:

$$a_w = \frac{H}{2} \frac{\cosh\,(2\pi(z + h)/L_w)}{\sinh\,(2\pi\, h/L_w)} \qquad (49)$$

The formula for this amplitude can be simplified in case of deep water waves and shallow water waves:

- deep water if h/L > 0.5
- shallow water if h/L < 0.05

The maximum horizontal particle amplitude in deep water waves:

$$a_w = \frac{H}{2} \exp^{2\pi . z/L_w} \qquad (50)$$

The maximum horizontal particle amplitude in shallow water waves:

$$a_w = \frac{H}{2} \frac{L_w}{2\pi\, h} \qquad (51)$$

Wave forces

The impact of waves on a floating screen is a complicated phenomena. In this chapter simple calculation methods are presented for the following extreme situations:

- waves which are relatively small compared with the length and the depth of a screen and
- waves which are relatively long compared with the length of a screen.

These calculation methods are based on a strong schematization of this phenomena.
In case of relatively small waves the calculation of the wave impact is based on pressures against the screen, and in case of long waves the wave impact is based on drag forces on the screen.

Short waves

The in this section presented design method is based on an analogy between rigid floating screens and vertical breakwaters. In the Shore Protection Manual (1973) a distinction is made between breaking and non-breaking waves. However, according to Goda (1985) the method of Minikin (1955, 1963) which had been proposed for breaking waves in the Shore Protection Manual, over-estimates the wave pressure forces. Based on hydraulic model investigations Ito (1966) and Goda concluded that the same method can be used for breaking and non-breaking waves. In the following this method is described.

The maximum wave height H_{max} of the incoming wave is

$$H_{max} = 1.8\ H_s \qquad (52)$$

in which H_s = significant wave height (m). The maximum wave height H_{max} is measured at some distance from a screen, at least 5 H_s (Goda, 1985), because partly a wave will reflect against a screen and partly it will be transmitted. The wave height that actually exists at the structure is the sum of H_{max} and the height of the wave reflected by the structure (H_r). The reflection coefficient r_{rf} is defined as $r_{rf} = H_r/H_{max}$. If it is assumed that a screen can follow the wave elevation of the water surface instantaneously without any limitation by the anchoring ropes, than overtopping of the floats will not occur.

The maximum elevation h_{max} to which the wave pressure is exerted is (see Figure 4.11):

$$h_{max} = \frac{1}{2}\,(1 + r_{rf})\,(1 + \cos\beta)\,H_{max} \qquad (53)$$

in which β = angle between the wave approach direction and a line perpendicular to the screen (degrees). The expression $(1 + \cos\beta)$ which accounts for the effect of oblique wave approach, is 1 for the case the waves approach the screen perpendicular. For design conditions Goda recommends in this formula $r_{rf} = 0.5$. In that situation with a sufficient deep screen than the height of the transmitted waves is about 0.4 to 0.6 of the incoming wave height. However, for a design of a screen it is recommended to consider a floating surface screen loaded by the incoming wave height h_{max} and assuming a horizontal water surface behind the screen.

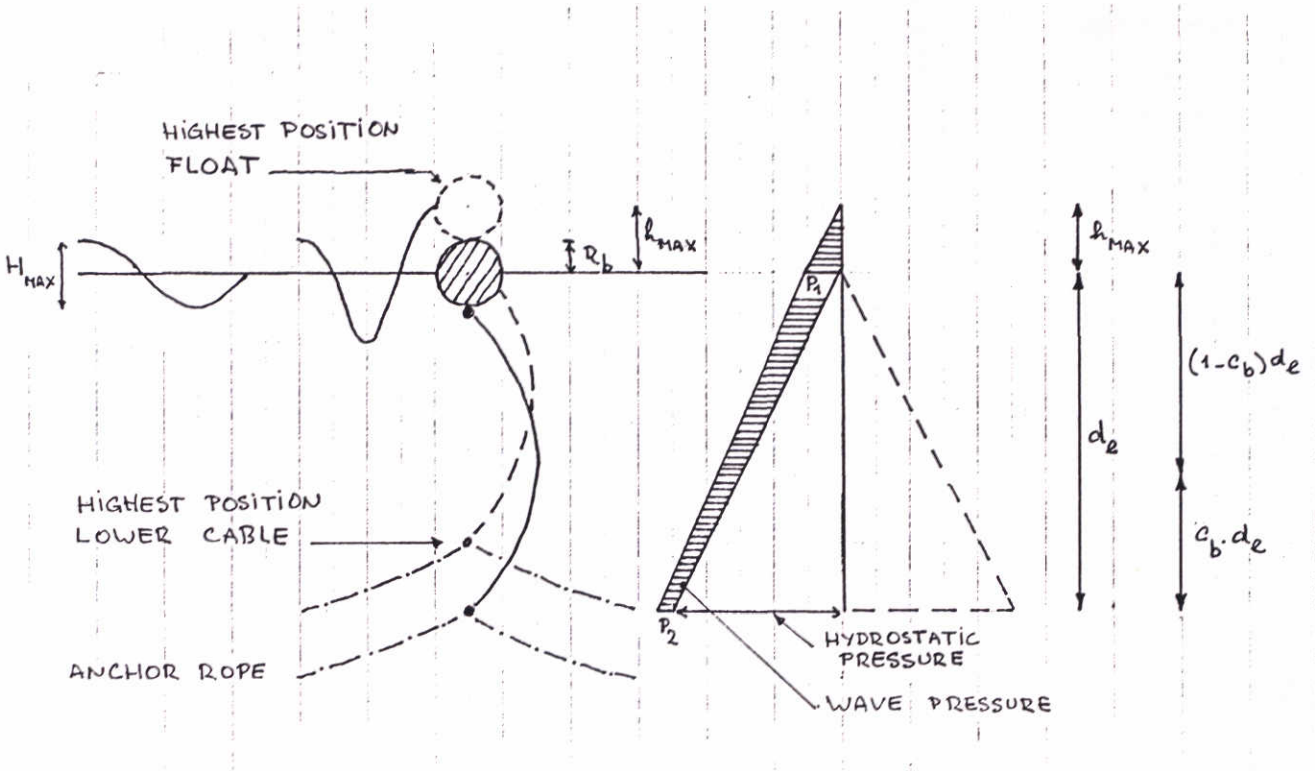

Figure 4.11 Calculation wave pressure on screen

The approach of Sawaragi (1989) for the calculation of wave forces on bottom screens is similar to the approach presented by Goda. The pressure on the screen is the sum of a permanent hydrostatic component relative to the still water level and a periodic component by the waves. The permanent hydrostatic pressure component in front of the screen is balanced by the permanent hydrostatic pressure behind the screen, see Figure 4.11. Therefore the hydrostatic forces do not contribute to the forces exerted on the screen.

In case $\beta = 0$ the wave pressure p_w varies over the depth as:

$$p_w(z) = \frac{1}{2}(1 + r_f)\,\rho\, g\, H_{max}\left[\frac{\cosh\,(2\pi(z + h)/L_w)}{\cosh\,(2\pi h/L_w)}\right] \qquad (54)$$

in which L_w = wave length (m).
The maximum wave pressure occurs at the still water surface z= 0 (Goda, 1985):

$$p_{w,max} = \frac{1}{2}\,(1 + r_f)\,(1 + \cos\beta)(a_1 + a_2\cos^2\beta)\,\rho\, g\, H_{max} \qquad (55)$$

in which

$$a_1 = 0.6 + \frac{1}{2}\left[\frac{4\pi h/L_w}{\sinh\,(4\pi h/L_w)}\right] \qquad (56)$$

$$a_2 = \text{minimum of} \quad \frac{h - d_e}{3h}\left(\frac{H_{max}}{d_e}\right)^2 \quad \frac{2d_e}{H_{max}} \tag{57}$$

The maximum wave pressure at the bottom edge of the screen:

$$p_w(z=-d_e) = \frac{1}{2}(1 + r_r)(1 + \cos\beta)(a_1 + a_2\cos^2\beta)\,\rho\, g\, H_{max}\,\frac{\cosh(2\pi(h - d_e)/L_w)}{\cosh(2\pi h/L_w)} \tag{58}$$

To calculate the wave force on the screen Goda proposed a simplified calculation by a straight interpolation between the maximum wave pressure at the bottom edge of the screen to the maximum wave pressure at the still water level and a straight interpolation between this maximum wave pressure at the still water level and the maximum elevation of the water surface, where the wave pressure is zero.

The wave force on the screen is

$$F_w = \frac{1}{2} p_{w,max} h_{max} + \frac{1}{2}(p_{w,max} + p_{w,z=-d_e})(d_e + r_b - h_{max}) \tag{59}$$

In which $p_{w,max}$, h_{max} and $p_{w,\,z=-de}$ are calculated with the previous formulas. In case d_e is not yet calculated than a first estimate with d_o and in a next calculation d_e should be substituted. F_w should be distributed over the lower cable and the upper cable:

$$F_{w,u} = \frac{(1 - c_b)\, d_e + r_b}{d_e + r_b} F_w \tag{60}$$

$$F_{w,l} = \frac{c_b\, d_e}{d_e + r_b} F_w \tag{61}$$

in which F_w = wave force per running meter of the cables.

The following extreme situations have to be distinguished for the upper cable:

screen system	*deformation of the upper cable*	*Wave force on the upper cable*
rigid	$\delta_{c,w}$ according formula 31 = 0	$F_{w,u}$ according formula 60
flexible	$a_w << \delta_{c,w}$	$F_{w,u} = 0$ the screen follows the particle movements induced by waves
flexible	$a_w >> \delta_{c,w}$	$F_{w,u} = c_i F_{w,u}$ according formula 60 dynamic wave impact after tightening of the screen

Table 4.4 The wave force as function of the flexibility and deformation of the upper cable.

A similar table can applied for the lower cable. When the screen is anchored slack in regular waves, it oscillates periodically in such a way that it is pushed forward and tightened up by waves in a half period of the motion and in turn is drawn back and tightened up again in the other half period. Directly after tightening of the screen, especially the upper and lower cables, the wave impact induces maximum peak forces in the screen system. In a physical model investigation Sawaragi (1989) had measured these peak forces in the upper and lower cable, see example in Figure 4.12. For each situation these peak forces can be different depending on the length of the screen and on the phase of the wave motion at the moment of tightening. Based on his results the following values are given $c_i = 2$ for a steel cable with a canvas screen and $c_i = 1.3$ for nylon cables with a canvas screen. These values need to be checked for a design calculation of a floating screen. This model investigation indicated that $F_w = 0$ if $a_w < 1.5\ \delta_{c,w}$.

The maximum deformation $\delta_{c,w}$ of a cable under wave loading is calculated by:

$$\delta_{c,w} = \frac{T_c}{F_w}\left[\cosh\left(\frac{F_w\ 0.5\ L_e}{T_c}\right) - 1\right] \qquad (62)$$

In the last two formulas $\delta_{c,w}$ and $T_{c,w}$ are the unknown parameters which can be solved together with the formula for the shape of the cables and Hooke's formula.

Translation waves can create a water level difference over the screen. This water level difference results in a force on the screen. This force is the difference of the hydrostatic forces on both sides of the screen. These waves can propagate in a direction parallel to the screen and acting on one side of the screen only. Translation waves propagating in a direction normal to the screen might partly reflect and partly pass the screen, depending on the length and the depth of the screen. This reflection also results in a water level difference over the screen and a resulting force on the screen.

If wave overtopping of a floating screen can occur, for example because of short anchor ropes, than the resulting force on the floats can be estimated with the results published by Goda (Goda, 1985).

Long waves

The waves forces on a rigid body can be calculated by Morison's equation, if the motion of the water particles in the waves is unaffected by the presence of the structure (floating screen) itself. This means that the characteristic dimensions (length of the screen) should not exceed 0.2 L, L = wave length. If the waves are smaller than the scattering of the waves by the structure should be calculated by a wave diffraction theory.

Morison's equation is based on the assumption that the wave force can be expressed as the linear sum of a drag force, due to velocity of water flowing around the body (e.g. screen), and an inertia force, due to acceleration of water.

$$dF(z) = C_D \frac{1}{2}\rho |(u(z) - u_s)|(u(z) - u_s)\, dA(z) + C_m\, \rho(u(z) - \dot{u}_s) dm(z) + (\rho\, dm(z) - dM)\, \dot{u}_s(z) \qquad (63)$$

$$F = \int dF(z) dz$$

in which:
M = mass of screen + added mass M_o (kg)
u_s = velocity of the screen (m/s)
ρ = density of water (kg/m^3)
The wave velocity u_w in (63) is calculated with formula (48), C_D = 1 to 2 and C_M = 1.5 to 2.5 (CIRIA, 1977). If more accurate values are required than these can be determined in a physical model investigation.
The maximum force is a combination of the drag force and the inertia force as function of 2π (x/L - t/T). Different values of this parameter can be presented in a table, where the maximum combination can be determined (see for example on pp 170 CIRIA UR8, 1977).
Silt Protector (Taiyo Kogyo Corporation) proposes to simplify this formula in the following way:

- neglect the inertia force,
- consider the screen as a rigid body, $u_s = 0$,
- integration over the depth of $\hat{u}_w$ in formula (48) results in a depth averaged flow velocity,

$$F_D = C_D \frac{1}{2}\rho \overline{u^2} \qquad (64)$$

in which F_D = drag force per surface unit (N/m^2). In general the first two simplifications introduce considerable inaccuracies in the calculated forces and therefore they are not recommended for a general design formula.

4.2.7 Oscillations and oscillating forces

Under certain conditions a floating screen might be sensitive for vibrations and/or oscillations. It is well known that steady flow normal to bluff cylinders produces regular vortex shedding, so-called von-Karman eddies. In steady flows vortices are shed alternately from either side of the cylinder producing an oscillating force across the stream, called lift force. In the flow direction in addition to a steady drag force there is a small fluctuating drag force associated with the shedding of individual vortices. The predominant frequency of this force is twice the frequency of the lift force.
For cylinder type of structures these forces can be calculated by (CIRIA, UR8, 1977):

$$F_D' = C_D' \frac{1}{2} \rho u^2 A \quad (65)$$

in which C_D' = root mean square of the fluctuating part of the drag coefficient = 0.15

$$F_L' = C_L' \frac{1}{2} \rho u^2 A \quad (66)$$

in which C_L' = root mean square of the fluctuating part of the lift coefficient = 0.4.

Vortex shedding can also be produced by wave action. The fluctuating forces which result and which direction is transverse to the direction of wave propagation, can be of a similar magnitude to the wave induced in-line forces on cylinders (CIRIA, 1977).

The flow separation at the lower edge of a floating screen can induce small scale oscillating forces or vibrations of the edge of the screen depending on the pretension of the lower cable.

In the literature no data has been found on oscillating forces on floating screens. From a theoretical point of view one should expect that these forces and oscillations also occur with floating screens, at least under certain conditions. Therefore it is recommended to increase the safety factor in the design calculations for these possible oscillating forces.

4.2.8 Wind force and wind set-up

Wind loads that part of the floats which is above the water surface. The wind induced force can be calculated by (see also Silt Protector, Taiyo Kogyo Corporation (1994)):

$$\sigma_{wi} = C_{D,wi} \frac{1}{2} \rho_{air} u_{wi}^2 A_{fl} \quad (67)$$

in which
σ_{wi} = the wind force (N/m'), A_{fl} = cross-section of that part of the float which is above the water surface and this cross-section is projected perpendicular to the wind direction (m^2/m'), ρ_{air} = density of air (kg/m^3), u_{wi}= wind velocity (m/s) and the drag coefficient $C_{D,wi}$ (-). In coastal areas of the Netherlands u_{wi} = 30 m/s, ρ_{air} = about 1 kg/m^3 and $C_{D,wi}$ = 0.8 are often recommended for design calculations.

Wind set-up can create a small water level difference over a floating screen, especially if a floating screen reaches to the bottom. In that case the resistance for the flow to pass the screen is sufficiently high to maintain a small water level difference over the screen. Wind set-up Δh can be calculated with a standard method.

$$\Delta h = c\, c_{shp} \frac{u_{wi}^2}{g} \frac{L_f}{h} \cos(\beta) \quad (68)$$

in which L_f = fetch length (m), β = angle between wind direction and normal to screen (degrees), c = (3 to 4) 10^{-6}, c_{shp} = shape factor for the influence of the banklines of the water body on wind set-up, in general c_{shp} = 1.

4.2.9 Density differences and floating debris

In case a floating screen is not loaded by a steady flow the temperature of the water in front of the screen and behind the screen can be different. This difference exerts a force F_t on the screen (Karelse, 1996):

$$F_t = \frac{1}{2} (\rho_{t_1} - \rho_{t_2}) \, g \, d_e^2 \qquad (69)$$

in which
$\rho(t_1)$ = density of water at temperature t_1 (kg/m^3)
d_e = effective depth of the screen (m)

In case of a difference in temperature and a difference in sediment concentration than the pressure difference on the screen is calculated by (69) in which $(\rho_{t,1}-\rho_{t,2})$ is replaced by $\Delta\rho_{t,sed}$ (Karelse, 1996):

$$\Delta\rho_{t,sed} = (1.0 - \frac{0.001\ c_{con_1}}{\rho_{sed}}).\rho_{t_1} - (1.0 - \frac{0.001\ c_{con_2}}{\rho_{sed}}).\rho_{t_2} + 0.001(c_{con_1} - c_{con_2}) \qquad (70)$$

in which
c_{con} = concentration of sediment (mg/liter)
ρ_{sed} = density of sediment (kg/m^3).
This pressure difference can be substituted in the following formulas:

$$\sigma_{c,d,u} = \frac{1}{6} \Delta\rho_{t,sed} \, g \, d_e^2 \qquad (71)$$

$$\sigma_{c,d,l} = \frac{1}{3} \Delta\rho_{t,sed} \, g \, d_e^2 \qquad (72)$$

in which
$\sigma_{c,d,u}$ = the force by different water temperatures and sediment concentrations per running meter of the upper cable (N/m')
$\sigma_{c,d,l}$ = the force by different water temperatures and sediment concentrations per running meter of the lower cable (N/m')
It is assumed that the density of sediment is the same at both sides of the screen and that this difference in sediment concentration and in water temperature is constant over the effective height of the screen (Karelse, 1996).

Floating debris causes a concentrated force at the floats and/or the upper layer of the screen. Especially in case wind and flow push debris against a screen.

4.2.10 Proposed calculation method

The hydrodynamic load on a screen with an upper and a lower cable can be calculated by the following formulas which have been described in the previous sections.

Forces
Steady flow induces a drag force and a lift force.
The drag force on the screen (N/m^2) is calculated by:

$$\sigma = C_D \frac{1}{2} \rho u^2 \quad (73)$$

The drag force (N/m') on the upper cable is calculated by:

$$\sigma_{c,u} = C_D \frac{1}{2} \rho u^2 (1 - c_b) d_e \quad (74)$$

in which
c_b varies between 0.3 and 0.5, default value 0.5. The value of c_b depends on the shape of the screen and on the velocity profile in the approach flow.
C_D varies between 1.5 to 2 for d/h < 0.3 and for d/h > 0.3 C_D can be estimated by:

$$C_D = (c + 12.3 (\frac{d}{h} - 0.27)^2) \cos \alpha + 0.15 \quad (75)$$

in which c varies between 2 and 3, default value 2.5

A steady flow induces also a lift force (N/m^2) on the screen:

$$\sigma_L = 0.2 \rho u^2 \quad (76)$$

The lift force (N/m') on the upper cable is calculated by:

$$\sigma_{c,L} = 0.2 \rho u^2 (1 - c_b) d_e \quad (77)$$

An impulsive force is distributed equally over upper and lower cable:

$$\sigma_{c,i,u} = \sigma_{c,i,l} = -\frac{1}{4} c_\omega c_{cur} \rho d_e^2 \frac{(\delta_c - u_o \Delta t)}{\Delta t^2} \quad (78)$$

in which values of the coefficients c_{cur} and c_ω can be read in Table 4.2.

Waves:
Long waves:

$$a_w = \frac{H}{2} \frac{\cosh (2\pi(z + h)/L_w)}{\sinh (2\pi h/L_w)} \quad (79)$$

in which $0.001 < H_s / L_w < 0.05$, default value $L_w = 25 H_s$
$0 < \delta_c < a_w$:

$$\sigma_{c,w,max} = \frac{a_w - \delta_c}{a_w} c_c \rho g \frac{H}{2} d_e \quad (80)$$

$\delta_c > a_w$:

$$\sigma_{c,w,max} = 0 \quad (81)$$

In the first calculation δ_c is assumed zero and in the next calculation δ_c has a realistic value.

Short waves:

The maximum wave height H_{max} of the incoming wave is

$$H_{max} = 1.8\ H_s \quad (82)$$

The maximum elevation h_{max} to which the wave pressure is exerted is

$$h_{max} = \frac{1}{2}(1 + r_{rf})(1 + \cos\beta)\ H_{max} \quad (83)$$

Default value $r_{rf} = 0.5$. In case $\beta = 0$ the wave pressure p_w varies over the depth as:

$$p_w(z) = \frac{1}{2}(1 + r_{rf})\ \rho\ g\ H_{max}\ [\frac{\cosh(2\pi(z + h)/L_w)}{\cosh(2\pi h/L_w)}] \quad (84)$$

The maximum wave pressure occurs at the still water surface z= 0:

$$p_{w,max} = \frac{1}{2}(1 + r_{rf})(1 + \cos\beta)(a_1 + a_2\cos^2\beta)\ \rho\ g\ H_{max} \quad (85)$$

$$a_1 = 0.6 + \frac{1}{2}[\frac{4\pi h/L_w}{\sinh(4\pi h/L_w)}] \quad (86)$$

$$a_2 = \text{minimum of } \frac{\frac{h - d_e}{3h}(\frac{H_{max}}{d_e})^2}{\frac{2d_e}{H_{max}}} \quad (87)$$

The maximum wave pressure at the bottom edge of the screen:

$$p_w(z=-d_e) = \frac{1}{2}(1 + r_{rf})(1 + \cos\beta)(a_1 + a_2\cos^2\beta)\ \rho\ g\ H_{max}\ \frac{\cosh(2\pi(h - d_e)/L_w)}{\cosh(2\pi h/L_w)} \quad (88)$$

$$F_w = \frac{1}{2}\ p_{w,max}\ h_{max} + \frac{1}{2}(p_{w,max} + p_{w,z=-d_e})(d_e + r_b - h_{max}) \quad (89)$$

F_w is distributed over the lower cable and the upper cable (N/m'):

$$\sigma_{c,w,u} = \frac{(1 - c_b)\ d_e + r_b}{d_e + r_b}\ F_w \quad (90)$$

The maximum deformation $\delta_{c,w,u}$ is calculated for the upper cable:

$$\sigma_{c,w,l} = \frac{c_b\, d_e}{d_e + r_b} F_w \qquad (91)$$

$$\delta_{c,w,u} = \frac{T_c}{\sigma_{c,w,u}} \left[\cosh\left(\frac{\sigma_{c,w,u}\, 0.5\, L_e}{T_c}\right) - 1\right] \qquad (92)$$

And a similar formula calculates the maximum deformation of the lower cable.

The following situations have to be distinguished for the wave force on the upper cable:

screen system	*Deformation of the upper cable*	*Wave force on the upper cable*
rigid	$\delta_{c,w,u} = 0$	$\sigma_{c,w,u}$ according to formula 90
flexible	$a_{w,u} << \delta_{c,w,u}$	$\sigma_{c,w,u} = 0$ the screen follows the particle movements induced by waves
flexible	$a_{w,u} >> \delta_{c,w,u}$	$\sigma_{c,w,u} = c_i\, \sigma_{c,w,u}$ according to formula 90, dynamic wave impact after tightening of the screen, default value $c_i = 2$

Table 4.5 The wave force as function of the flexibility and deformation of the upper cable.

In this table the particle amplitude a_w is calculated by (79) with $z = 0$ for the upper cable and $z = -d_e$ for the lower cable. A similar table can be prepared for the lower cable.
The force $\sigma_{c,d,u}$ (N/m') on the lower cable induced by density differences:

$$\sigma_{c,d,u} = \frac{1}{6} \Delta\rho_{t,sed}\, g\, d_e^2 \qquad (93)$$

The force $\sigma_{c,d,l}$ (N/m') on the lower cable induced by density differences:

$$\sigma_{c,d,l} = \frac{1}{3} \Delta\rho_{t,sed}\, g\, d_e^2 \qquad (94)$$

in which

$$\Delta\rho_{t,sed} = \left(1 - \frac{0.001 c_{con}}{\rho_{sed}}\right) \rho_{t_1} - \left(1 - \frac{0.001\, c_{con}}{\rho_{sed}}\right) \rho_{t_2} + 0.001\, (c_{con,1} - C_{con,2}) \qquad (95)$$

The wind on the floats causes a force (N/m') on the upper cable:

$$\sigma_{c,wi} = C_{D,wi} \frac{1}{2} \rho_{air}\, u_{wi}^2\, A_{fl} \qquad (96)$$

The dimensioning of a screen should be based on a combination of the different loads, depending on the location of the screen. If all different loads are independent of each other, than the design load is the sum of the loads:

for the upper cable:

$$\sigma_{c,u} = \sigma_{u,u} + \sigma_{c,L,u} + \sigma_{c,i,u} + \sigma_{c,w,u,max} + \sigma_{c,d,u} + \sigma_{c,wi} \quad (97)$$

The total force on the lower cable is calculated with a similar formula, except the contribution of the wind on the floats.

Screen
The proposed calculation method for a screen starts with the assumption of a value of the angle, Θ, of the edge of a screen where it is connected with the upper cable and to use d_o as a first estimate of d_e. In a schematic approach the total load on upper and lower cable is distributed equally over the screen:

$$\sigma = \frac{(\sigma_{c,u} + \sigma_{c,l})}{d_o} \quad (98)$$

The resulting force T_s is estimated by:

$$T_s = (1 - c_b)\ \sigma\ d_o \frac{1}{\sin\theta} \quad (99)$$

Calculate σ_s:

$$\sigma_s = \frac{2\ T_s}{d_o\ (1 + \frac{T_s}{A_s\ E_s})} \tan\theta \quad (100)$$

Calculate d_e :

$$\sinh(\frac{\sigma_s\ d_e}{2\ T_s}) - \tan\theta = 0 \quad (101)$$

Repeat the calculation of T_s and σ_s with d_o replaced by d_e.
Calculate d:

$$d = d_o + \frac{T_s\ d_o}{A_s\ E_s} \quad (102)$$

Calculate the maximum sag of the screen:

$$\delta_{s,max} = \frac{T_s}{\sigma_s} [\cosh\frac{\sigma_s\ d_e}{2\ T_s} - 1] \quad (103)$$

Repeat this calculation for different values of angle Θ of the edge of the screen (= where the screen is connected with a cable) and select from the calculated results a design value of Θ. For an unequal distribution of the maximum force over the length of the screen a safety factor, for example 2, is recommended.

Cables
The forces and deformations of the cables are characterized by the unknowns T_c, L, L_e and δ_c which can be calculated by the following formulas. First a value of angle α has to be selected. An approximation of T_c in the upper cable is obtained by formula (104) where L_o

is an approximation of L_e.

$$T_c = \frac{1}{2}\,\sigma_{c,u}\,L_o\frac{1}{\sin\alpha} \tag{104}$$

An approximation of σ_c is calculated by:

$$\sigma_c = \frac{2\,T_c}{L_o\,(1 + \frac{T_c}{A_c\,E_c})}\tan\alpha \tag{105}$$

The effective length L_e is calculated by:

$$\sinh(\frac{\sigma_c\,L_e}{2\,T_c}) - \tan\alpha = 0 \tag{106}$$

The calculation of T_c and σ_c should be repeated with L_e instead of L_o.
The elongation of the cable is calculated by:

$$L = L_o + \frac{T_c\,L_o}{A_c\,E_c} \tag{107}$$

The maximum sag of the cable is calculated by:

$$\delta_c = \frac{T_c}{\sigma_c}\,(\cosh\frac{\sigma_c\,L_e}{2\,T_c} - 1) \tag{108}$$

The values of α mentioned in Table 4.6 are recommended for design calculations.

α	*tan* α
(degrees)	(-)
16.7	0.3
21.8	0.4
26.6	0.5

Table 4.6 Recommended values for angle α.

These four formulas (104) to (108) can be used for the upper cable as well for the lower cable.
In the calculation of the hydrodynamic loads the screen had its initial position, characterized by d_o and L_o. Now the whole calculation can be repeated with effective screen area (d_e and L_e). This recalculation starts with the hydrodynamic loads.

4.2.11 Example

An example of the proposed calculation method has been elaborated for the case of a screen loaded by a steady flow and by waves. The flow velocity and wave height have been varied. The constant parameters are summarized in Table 4.7.

Waves	
direction	0 degrees
reflection coefficient	0.5
Steady flow	
density	1000 kg/m^3
C_D	3.3
Screen	
water depth	10 m
depth d_o	5 m
coefficient c_b	0.5
length L_o	20 m
Thickness	0.001 m
Elasticity modulus	3.10^9 N/m^2
θ	45 degrees
Radius float	0.75 m
Upper cable	
A_c	0.0005 m^2
Elasticity modulus	7.10^9 N/m^2
angle α	30 degrees

Table 4.7 Constant parameters in the example

Five combinations of steady flow attack and wave attack have been selected, see Table 4.8. In this table $F_{w,u}$ is the force exerted by the waves on the upper cable and $F_{D,u}$ is the drag force exerted by the steady flow on the upper cable.

Waves			*Steady flow:*	
wave height (m)	wave length (m)	$F_{w,u}$ (10^3 N/m')	u (m/s)	$F_{D,u}$ (10^3 N/m')
1.5	37.5	10.7	0.7	2.0
1	25	8.8	0.5	1.0
0.5	12.5	5.5	0.4	0.66
0.25	6	3.0	0.3	0.37
0.2	5	2.4	0.2	0.16

Table 4.8 The varied parameters, wave height and flow velocity

The response of the screen to the steady flow only is presented in Table 4.9. This response is the result of the first calculation step. In a next iteration the drag force is calculated by formula based on the effective depth instead of the initial depth of the screen.
The very small elongation of the screen indicates that the membrane is too thick for this steady flow attack.

Flow velocity	T_s	d_e	δ_{max}	d	d/d_o
(m/s)	(10^3 N)	(m)	(m)	(m)	(-)
0.7	2.5	4.410	1.036	5.0042	1.000
0.5	1.3	4.409	1.036	5.0022	1.000
0.4	0.83	4.408	1.036	5.0014	1.000
0.3	0.46	4.408	1.036	5.0008	1.000
0.2	0.21	4.407	1.036	5.0003	1.000

Table 4.9 Response of the screen to steady flow

The response to the combined wave and flow action on the screen shows that the elongation of the screen is very small, see Table 4.10. It can be considered to reduce the thickness of the screen. The deformation of the screen does not vary much for different loads and the force in the membrane increases considerably with increasing loads.

Flow velocity	*wave height*	a_w	T_s	d_e	δ_{max}	d	d/d_o
(m/s)	(m)	(m)	(10^3 N)	(m)	(m)	(m)	(-)
0.7	1.5	0.80	8.0	4.42	1.038	5.013	1.003
0.5	1	0.51	6.1	4.42	1.038	5.010	1.002
0.4	0.5	0.25	3.8	4.41	1.037	5.006	1.001
0.3	0.25	0.13	2.1	4.41	1.036	5.003	1.001
0.2	0.2	0.10	1.6	4.40	1.036	5.003	1.001

Table 4.10 Response of the screen to the combined action of flow and waves

The response to the combined wave and flow action on the upper cable:

Flow velocity	*wave height*	T_c	L_e	δ_c	L	L/L_o
(m/s)	(m)	(10^3 N)	(m)	(m)	(m)	(-)
0.7	1.5	622	22.48	3.16	23.55	1.17
0.5	1	461	21.54	3.03	22.63	1.13
0.4.	0.5	279	20.54	2.89	21.59	1.08
0.3	0.25	146	19.82	2.79	20.83	1.04
0.2	0.2	110	19.63	2.76	20.63	1.03

Table 4.11 Response of the upper cable to the combined action of waves and flow.

These are first calculation steps and should be followed by at least one more iteration step. However, these calculations are very usefull for a preliminary design of floating surface screen. The calculated deformation of the screen and the cables are a good indication for the need to optimize the thickness, the elasticity of the membrane and the cross-section and the elasticity of the cables, because in many situations the maximum acceptable deformation of a floating surface screen can be determined roughly by engineering judgement.

4.3 References floating screens

Christensen, B.S. and L. Kock (1997), Silt curtains, design criteria and practical application especially for ROBOOM silt curtains, CEDA dredging days, Amsterdam

Goda, Y. (1985) Random seas and design of maritime structures, University of Tokyo Press

Hallam, M.G., N.J. Heaf and L.R. Wootton (June 1977), Report UR8, Dynamics of marine structures: methods of calculating the dynamic response of fixed structures subject to wave and current action, CIRIA Under Water Engineering Group, London

Hoekstra, A. and C. Kooman (1969), Afsluiting Volkerak, M878 Deel IV Wind en stroom weerstand caisson en Deel V Krachten door de stroom op caissons tijdens plaatsings manouvres, Delft Hydraulics (Dutch)

Huis in 't Veld et al (1987), The Closure of tidal basins, Delft University Press, Delft

Ito,Y., M. Fujishima and T. Kittani (1966), On the stability of breakwaters, Rept. Port and Harbour Res. Inst., Vol. 5, No. 14, pp 134 (in Japanese) or Coastal Engineering in Japan, Vol. 14, 1971, pp. 53-61

Karelse, M. (1996) Een flexibel separatiescherm in een drinkwaterbekken, Thesis for Master of Science degree in Civil Engineering, Technical University Delft, Delft

Milgram, J.H. (1971) Forces and motions of a flexible floating barrier, Journal of Hydronautics, Vol. 5, Number 2, April 1971, pp 41 - 51

Minikin, R.R. (1963) Winds, waves and maritime structures:Studies in harbour making and in the protection of coasts, 2nd rev. ed., Griffin, London, pp 294

Nakamura Y. and T.Mizota (1971) Aerodynamic characteristics and flow patterns of a rectangular block, Report of Research Institute for Applied Mechanics, Kyushu University, Japan

Sawaragi, T., S.Aoki and H. Liu (1992) Wave-induced impulsive forces in tension cables of a floating silt curtain, Proceedings second International Offshore and Polar Engineering Conference ISOPE, Vol. 3, No 2, pp 243 - 265

Sawaragi,T., S.Aoki and A.Yasui (1989) Tension on silt curtains in currents and waves, Eight International Conference on Offshore Mechanics and Arctic Engineering, The Hague 19-23 March pp 13 - 21

Taiyo Kogyo Corporation (1994), Design of Silt protector, commercial brochure, Japan

US Army Coastal Engineering Research Center, (1973), Shore protection manual, Volume II, Section 7.3

5 Bottom screens

5.1 Constructional aspects

Bottom screens have been applied at one hand to prevent different phenomena, such as: siltation, transportation of suspended silt or bank erosion and at the other hand to stimulate local siltation. Siltation in a harbor has been prevented by a single screen in the mouth of a harbor. The transportation of suspended silt due to dredging activities has been prevented by a silt container, see Figure 5.1. Local sedimentation of sediments has been increased by a field of short screens, see sketch in that figure. Sometimes bottom screens have been used in combination with floating surface screens.

Different types of bottom screens:

- A geotextile bordered by upper and lower steel cables, floats are attached to the upper steel cable separately. The upper cable is connected to anchor lines and the lower cable has been sewn in the membrane material (Silt Protector, the same system has been developed as floating screen which has been described in the previous chapter).
- A pilot bottom screen made of a geotextile connected to two parallel sand-filled tubes as foundation of the bottom screen. Each float is 4 m long and it has an diameter of 0.5 m (Public Works Rotterdam, 1987)
- A pilot bottom screen made of geotextile with sewn in a polyester tube as float and a iron tube (eventually sand filled) as ballast. The screen has been anchored by concrete blocks. The units have a length of about 6 m (DHV, Meghna Estuary Studies, verbal communication).
- Pilot bottom screens made of permeable screens of woven geotextile. Each screen has a length of 3 m and a height of 1 to 2 m. A self-standing screen is connected with floats with a diameter of 0.2 m (Huygens, Verhoeven, de Wachter). They tested a field of 7 rows and each row has 5 sections.
- A Berosin bottom screen anchored in the bed at three sides by hydraulic anchors and one side connected with floats (Bureau van der Hidde).

These bottom screens have been applied in water depths up to 15 m. Silt Protector has designed screens for a maximum wave height of 1.5 m.

Materials used to construct a bottom screen are for example geotextiles made of polyester or polyamide. The screen can be made of a rubber canvas, a sand tight or permeable woven fabric, locally strengthened by belts. The floats are made from foam blocks in a polyethylene shell, or from standard tubes made from polyester, pvc or iron. These foam blocks consist of polyurethane or polystyrene. To make one large screen of a few hundred meters length sections have been interconnected by divers.

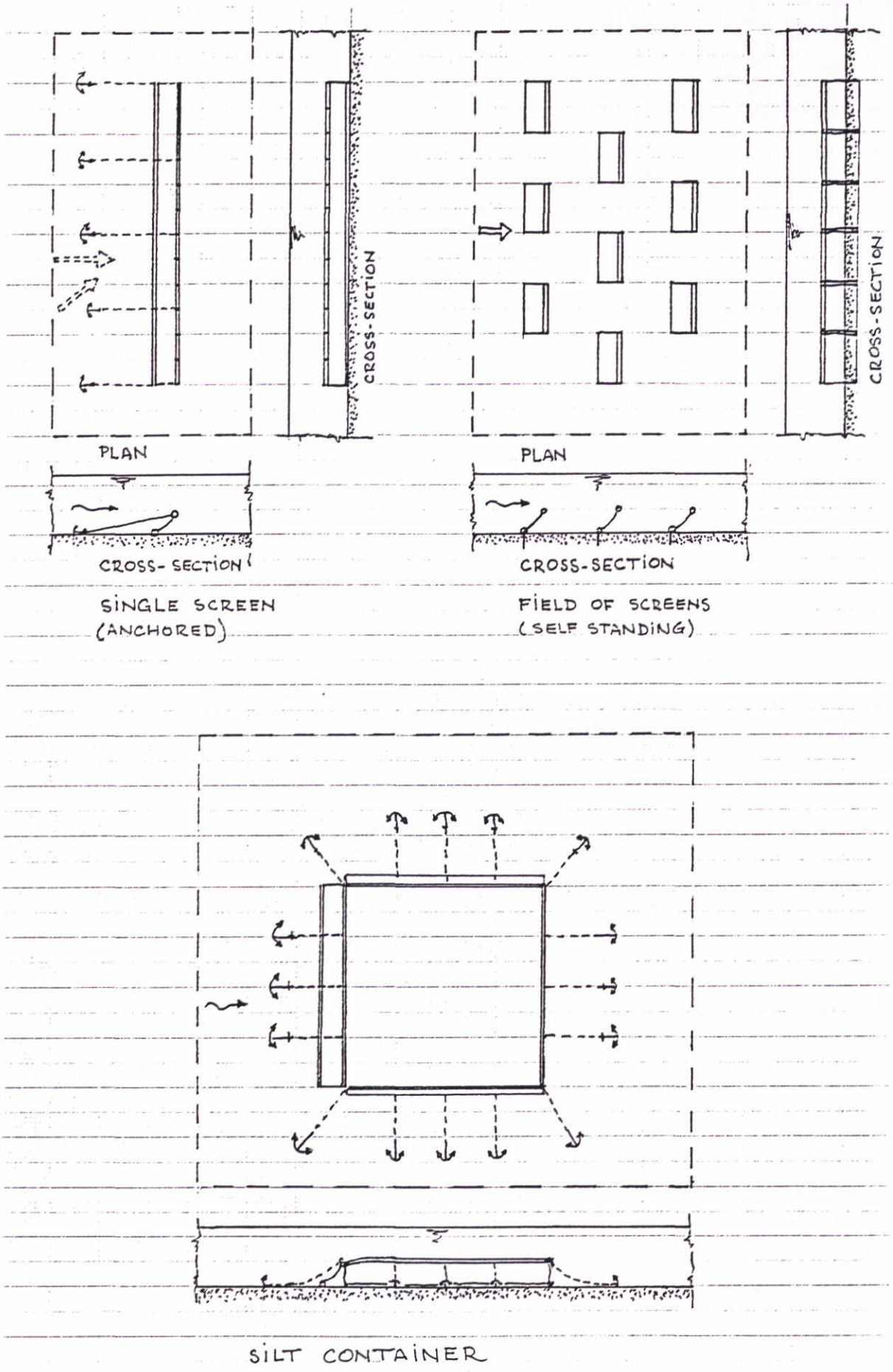

Figure 5.1 Different types of bottom screens

The life time of a screen is important for the design because the strength of a geotextile gradually deteriorates. Tests with polyester samples in sea water has shown a 5 to 40 % deterioration of the tensile strength and 5 to 35 % deterioration of the elongation after one year immersion (Silt Protector). In sea water screens have been used successfully as temporary structures with a life time less than one year. In general this deterioration of the strength depends on the type of synthetic material and deterioration by sun light can be prevented by extra protection.

In pilot tests with bottom screens several problems have been encountered, such as: screens damaged by passing ships (propeller action and anchors), broken sewn seams of the geotextile placed in a tidal environment with considerable wave action, geotextiles broken near the foundation placed in a coastal zone. These experiences show that a bottom screen needs to be designed carefully. In storage reservoirs screens have been applied also where the hydrodynamic load on a screen is less severe than in coastal zones, rivers and harbors.

Alternative constructions are made of strands of material (artificial seaweed). These have used for scour protection or for stimulation of local sedimentation.
In some cases a pile of sausages filled with sand functions as a permanent bottom screen. These sausages with a diameter of 0.5 to 1 m are made of synthetic geotextiles.

5.2 Calculation method

5.2.1 Introduction

In principle the proposed calculation method for bottom screens follows the same steps as the calculation method for floating screens as presented in the previous chapter. To prevent to much repetition only formulas related to special aspects of a calculation method for bottom screens have been presented in this section; first some aspects related to a bottom screen in a steady flow (Section 5.2.2) and next a bottom screen exposed to wave action (Section 5.2.3). Experiences with pilot project to test bottom screens have been described in Section 5.2.4.

In a steady flow a bottom screen deflects the approaching bottom flow to the upper layers and partly to both sides of the screen. Upstream of the screen a horse shoe vortex can develop, see Figure 5.2. Flow separation at the sides of the screen can create von Karman's eddies and vortex streets behind the screen depending on the length/height ratio of the screen. These vortices induce considerable lateral forces in the screen. Flow separation at the upper side of the screen induces small vibrations in the screen. These vibrations create small fluctuations in the forces in the screen.
In a riverine estuary a salt water wedge comes in under the fresh water carried by the river. A bottom screen can be loaded by the flow in a salt water wedge near the bottom and the opposite flow in the fresh water layer on top of it. This can result in a complicated deformation of a bottom screen.

Wave action induces changing forces in a screen. The shape of the screen changes also. Fatigue-properties of the screen geotextile can be decisive for the design. Wave action combined with a steady flow can result in a complicated flow pattern. In the following calculation method this flow pattern has been simplified.

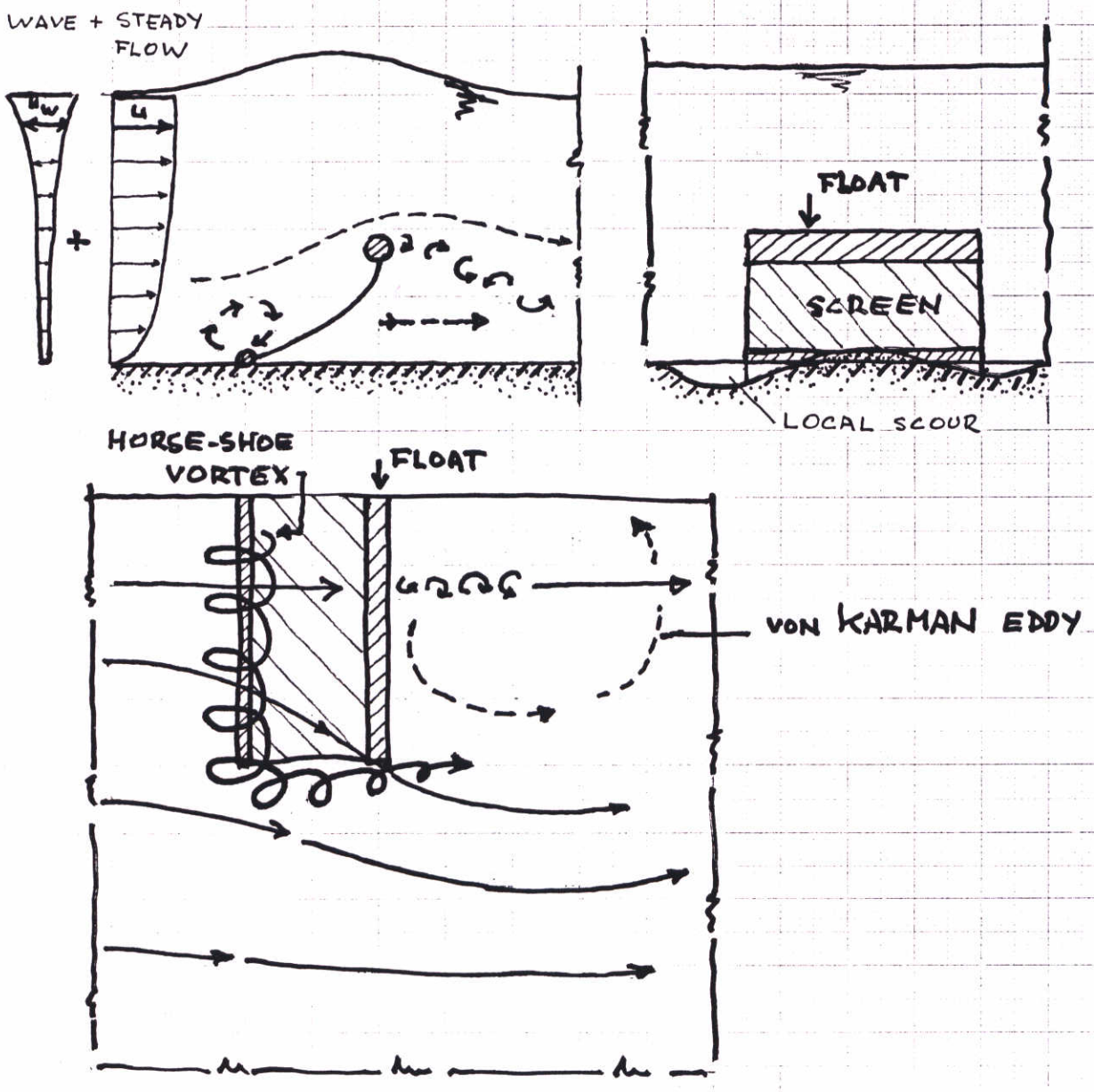

Figure 5.2 Flow pattern around a screen

5.2.2 Screen in steady flow

In a steady flow a boundary layer develops near the bed. The hydrodynamic load on 1 m^2 of a screen, see Figure 5.7:

$$\sigma_s = C_D \frac{1}{2} \rho u^2 \qquad (109)$$

in which C_D = a drag coefficient (-), ρ = density of water (kg/m^3), u = flow velocity (m/s). In a physical model investigation a screen had been tested in flume showing that C_D = 5 (Gemeentewerken Rotterdam, 1980).
This load is perpendicular to the screen. Since the flow velocity has a strong gradient near the bed the calculation should be done in slices with the flow velocity averaged over the thickness of a slice.

Silt can be transported in a bottom layer with an extremely high concentration of fine particles, which behaves as a Newtonian liquid and can move as a highly mobile density current along flat bottom slopes. Bottom screens can be applied to prevent the transportation of silt in such a density current (Public Works Rotterdam, 1987). Consider the situation that such a bottom layer loads a screen on one side and on the other side only clear water loads the screen. The force exerted by a silt layer on a screen is calculated by:

$$F_{slt} = \frac{1}{2} \overline{(\rho_{slt} - \rho_w)}\, g\, d_e^2 \qquad (110)$$

in which
ρ_{slt} = density of silt (kg/m^3)
ρ_w = density of water (fresh or saline) (kg/m^3)
d_e = effective height of a bottom screen (m)
This force acts perpendicular to a screen and it has to be combined with the hydrodynamic load (109) to a total force.

In general a float of a screen has been made of units with a circular cross-section. The upward force on a float per unit length is calculated by formula:

$$F_b = (\rho_w - \rho_b)\, g\, \pi\, r_b^2 \qquad (111)$$

in which
ρ_b = density of the float (kg/m^3)
r_b = radius of the float (m)

This force F_b makes equilibrium with the tension T_s in the screen. If the drag force by the flow on the float cannot be neglected than the vector sum of F_b and this drag force makes equilibrium with T_s.

The densities of different materials used for screens, cables and floats are listed in Table 5.1.

Material	*Density (kg/m^3)*
polyethene	930
polystyrene	1060
nylon	1140
pvc	1300
polyester	1400

Table 5.1 Densities of different materials used for bottom screens.

The size of the float can be designed if the maximum allowed forces in the screen are given or if the maximum movement of the screen is given. For example the bottom screen in the Botlek harbour basin should be lowered maximum 1 m if the screen is loaded by the maximum drag force. This condition was necessary to obtain a sufficient overall efficiency of the screen. The physical model investigation (Gemeentewerken Rotterdam, 1980) indicated a relation between the lowering of the screen and the angle of the screen near the bottom, see Figure 5.3. This relationship has been used in the design of the screen.

Calculation of the friction force caused by the flow along the screen and the pressure force against the bottom part of the float showed that these forces can be neglected compared with the floating force (Gemeentewerken Rotterdam, 1980).

A bottom screen should be anchored to the bed by separate anchor lines connected with the screen just under the float. To save some costs of such an anchoring system alternative systems have been tested in the field. If the flow and wave conditions are very moderate than the anchor lines can be omitted and the bottom screen can be anchored by only ballast sausages resting on the bed. However, the holding force of such a simple and cheap anchoring should not be overestimated. An other alternative anchoring system for small screens is to drill the geotextile directly into the bed. If the screen is loaded by wave action than fatique properties of the geotextile just near the bed where the geotextile is clenched in the bed should be sufficient to prevent coming apart of the geotextile.

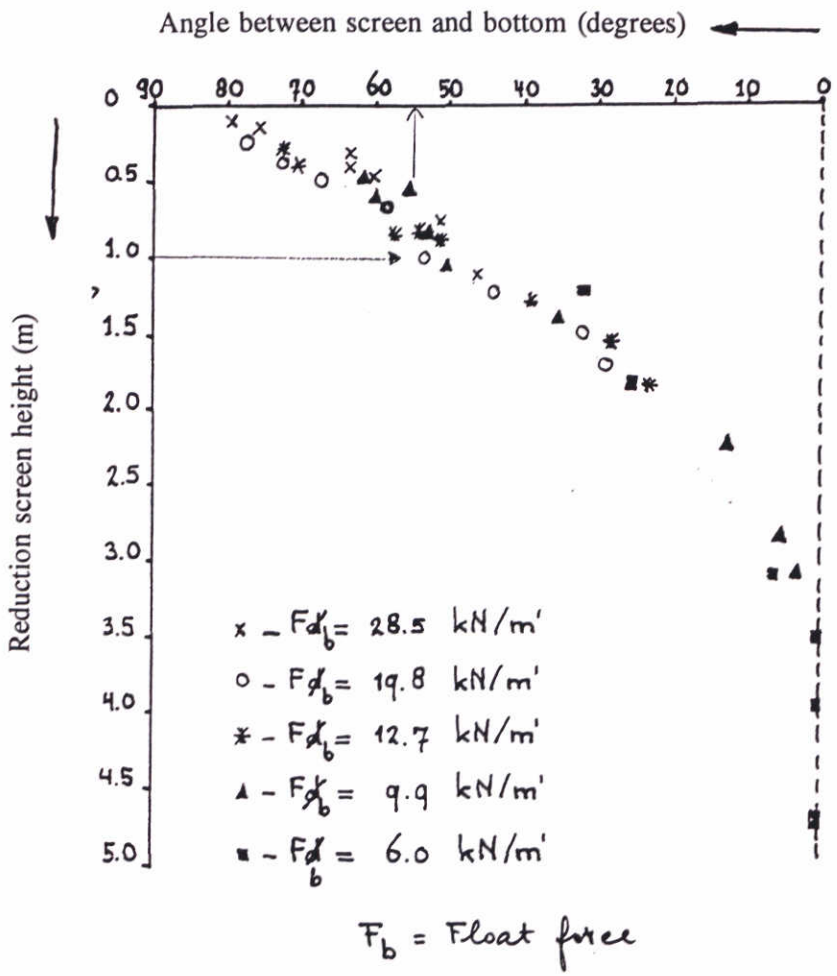

Figure 5.3 Experimental relationship between angle between screen and bottom and the lowering of the screen

5.2.3 Screen in waves

Sawaragi et al (1989) have tested a bottom screen in a physical model. In the analysis of the results he proposed to relate the forces in the screen near the bottom F_b as a linear function of the hydrodynamic pressure due to waves, integrated from the bottom to the top of the

screen. The pressure force P_{max} due to waves is according Sawaragi etal (1989):

$$P_{max} = \frac{\rho_w g H}{2 k} \frac{\sinh kd}{\cosh kh} \quad (112)$$

in which
h = water depth (m)
d = height of the screen (m)
H = wave height (m)
k = wave number, $2\pi/L_w$ (-)
ρ_w = density of water (kg/m^3)
g = acceleration by gravity (m/s^2)

The horizontal and vertical forces ($F_{s,h}$ and $F_{s,v}$ respectively) in the screen F_s near the bottom are:

$$F_{s,h} = c_h \frac{F_b}{\rho g d h} P_{max} \quad (113)$$

in which
c_h = empirical coefficient, about 0.7 (-).
F_b = buoyancy force of the float (N/m')

$$F_{s,v} = c_v \frac{F_b}{\rho g d h} P_{max} \quad (114)$$

in which c_v = an empirical coefficient, about 0.2 (-).
These results have not been verified with field testing. Therefore the application of these formula should be restricted to projects where also other design rules are applied. In general the maximum forces in a bottom screen occur near the bottom.

The combination of a surface screen and a bottom screen have been tested in a stationary flow in a physical flume model (Kano etal, 1989). Two different arrangements have been tested: the bottom screen upstream of a floating screen or in a downstream position. The differences in the flow pattern were small.

5.2.4 Experiences with bottom screens

5.2.4.1 Introduction

In the literature 1 well-developed application and 4 different pilot tests with bottom screens have been documented. The set-up and the purpose of each test was very different of each other. Therefore the most important results of these tests have been high-lighted in a separate summary of each test.

5.2.4.2 Silt screen in harbour

The basins of the harbour of Rotterdam need regular maintenance dredging to maintain sufficient depths for ships. Previously the dredged material had been used as soil fertilizer. But pollution had decreased the quality of this material and it had to be treated as a harmful waste material. This had increased the costs of maintenance dredging considerably and the harbour authorities planned some measures to reduce the sedimentation in their harbour basins.

The low flow velocities in the basins cause the transported sediment, mainly silt, to settle. Sediment is transported by the flow and 'normal' sediment concentration verticals have been measured. However, part of the sediment is transported as a fluid mud layer near the bottom of the basin. This mud layer has a thickness ranging from a few centimeters to several meters. This layer behaves as a Newtonian liquid with typical flow velocities of 0.1 m/s. The density of this layer is rather high, 1060 to 1230 kg/m3, because of the high sediment concentration. Different types of screens have been proposed to reduce this sedimentation, especially by mud flows.

Important design aspects of a silt screen and design conditions are:

- A bottom screen is effective if the height of the screen is about 50 % of the water depth. It was expected that such a screen should reduce maintenance dredging with 15 to 35%.
- In- and outgoing ships should pass the screen. It means a screen has to be lowered or removed sideways within about 10 minutes.
- A lowered screen should be protected against ship anchors sliding over the bottom.
- Maintenance dredging should be possible close to the screen or other measures should prevent sedimentation near the screen itself.
- If a screen is designed in sections than leakage through joints should be prevented.

The behavior of a bottom screen has been tested in several physical model investigations.

A single bottom screen has been selected and a pilot test screen has been constructed, see Figure 5.4. The screen is kept in upright position by floats. The material of the screen is polyester/polyamide sand tight woven fabric with a strength of 200 kN/m' in warp and 100 kN/m' in weft. No information on aging and fatigue has been found in the available design reports. In the final design the screen has been connected to a foundation and it can be removed sideways to allow ships to pass. The whole screen can be inspected and repaired on the dry river bank.

The foundation of a removable bottom screen is expensive compared with the cost of a screen. The design condition was that the screen should tear or break before the foundation would be damaged. Therefore the design engineers selected a screen with a low strength. The installation of the screen has been halted when at first ship contact several floats had been severed from the pilot screen. The authorities considered this damage as a failure of the test and a planned continuation of the test next year had been cancelled.

The exact reason of the damage is not known because no observations have been made during evenings and nights after the installation of a pilot screen. It is assumed that ship anchors had severed the floats. The size of the test would have justified continuous monitoring in a period of several weeks after installation. The safety factor in the design was 25% which is very low compared with a safety factor of 1000% recommended by Taiyo Kogyo Corporation for the design of Silt Protector screens.
Lack of field measurements resulted probably in a deterministic approach for the design conditions. In the Botlek basin complicated hydraulical and morphological phenomena occur. Probably more detailed frequency distributions of flow velocities over the vertical, ship induced water motion, long wave phenomena and density currents would have resulted in a probabilistic approach and more accurate design conditions.

References:

Hoedt, G. den, H.E. Metz, M. Veltman, W.Voskamp, Cost-effective reduction of sedimentation and maintenance dredging using geotextile flow diversion screens
Second International Conference on Coastal and port Engineering in Developing Countries, 1987

Delft Hydraulics, Application of silt screens to reduce sedimentation in access channels, R1158,

Delft Hydraulics, Vermindering slibbezwaar Botlekhaven, R2004, Juni 1984

Gemeentewerken Rotterdam, Ingenieursbureau Havenwerken, De ontwerp-sterkte berekening van het slibscherm, 69.30-R8004, April 1980

Ingenieursbureau Havens, slibscherm, deel 4, Onderzoekconstructie mogelijkheden dicht slibscherm, 69.30-R7801, Oktober 1978

Pilot test

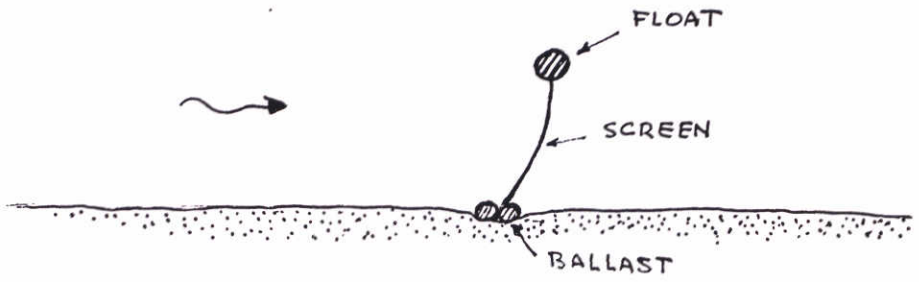

Final design

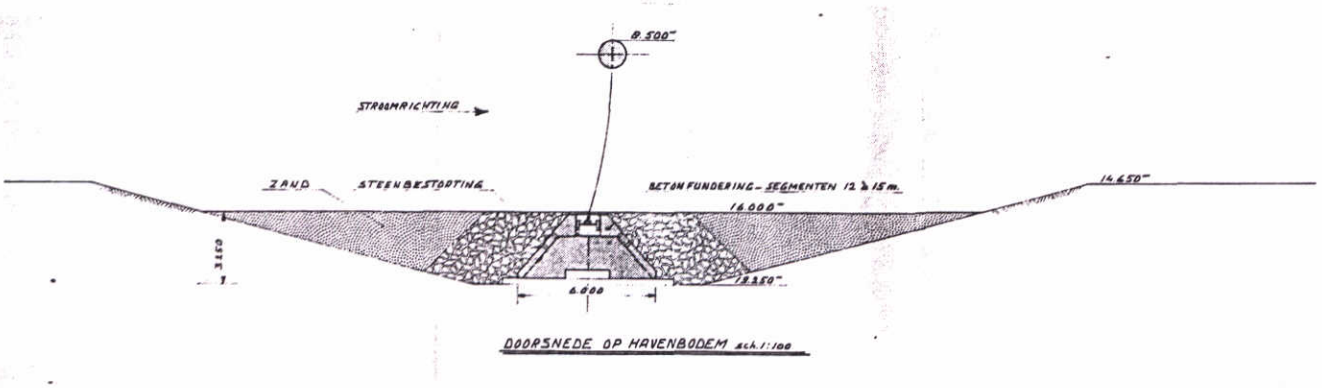

Figure 5.4 Silt screen in Botlek harbour, Rotterdam

5.2.4.3 GESEP bottom screens

The continuous regression of the beach at Knokke-Heist is the result of the netto transport of sandy beach material offshore by wave-induced underflow. This material is transported towards a tidal gully where the longshore tidal flow removes this material. A field of under water screens of the type GESEP (Geotextiles for Sea Bottom Protection) has been tested to intercept this offshore directed sediment transport, see Figure 5.5.

A research project has been set up to investigate this protection system. The University of Ghent has investigated the behaviour of bottom screens made of a netting of polyamide and UCO cloth in physical models to study:

- the behaviour of permeable screens of woven geotextile in steady flow,

- the erosion and deposition around the bottom screens,
- the impact and the behaviour of the screens under a combination of waves and flow.

In addition to these investigations the overgrowth of permeable geotextile has been tested in situ.

The optimal dimensions of a screen have been selected (a height = 1.5 m and width 3 m) with an inital mesh size of a screen fabric 0.1 by 0.1 m^2, see example in Figure 5.5. In the field test the screens have been placed at a lateral interdistance of 1.5 m and the distance between the 5 rows of screens is 4 m (in the main flow direction).
The flow velocity reduces locally in the shadow of a screen section to 40%. The length of the shadow area is about 4 times the height of a screen. In unidirectional flow the bed eroded upstream of the screens and deposited in the field of screens where a transverse dune developed. In general a combination of waves and flow introduce locally extra sediment transport which is caught in sedimentation areas and dunes elsewhere. In the neighbourhood of the field of bottom screens the sea bed is in a morphological equilibrium. If the field of screens is located near the offshore ends of groynes the screens initiate wave breaking which increase the beach erosion under normal conditions, but during severe stroms some of the collected sand in the field of screens is deposited at the beach. The field testing has been terminated after the screens had been broken near the sea bed because frequent bending of the screen (probably fatigue-phenomena).

References:

Huygens,M., R.Verhoeven, D.de Wachter (1994) and

Huygens,M., R.Verhoeven, D.de Wachter, J.Himpe, S.Buyck, F.Wens, B de Putter and P. de Wolf (1995)

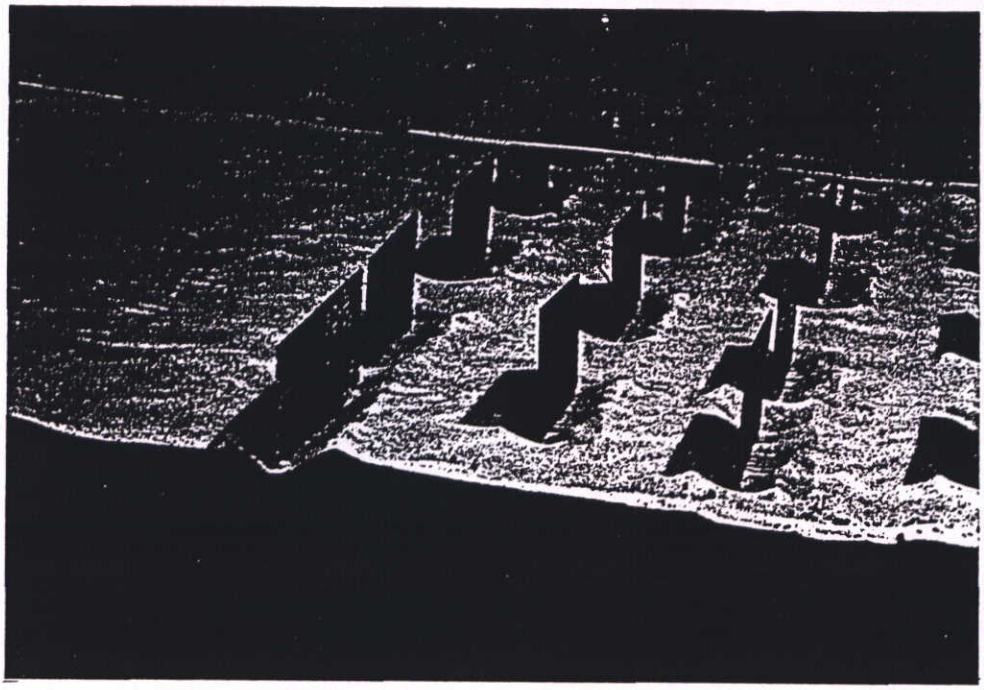

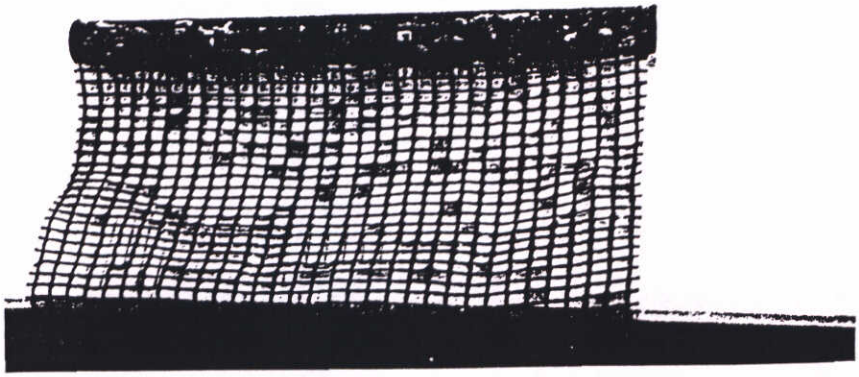

Figure 5.5 Model of GESEP screen

5.2.4.4 Silt Protector

Dredging work by a grab dredger can cause diffusion of polluted bottom soil by the induced extra turbulence over a large area. Polluted bottoms are found especially in urban areas and in existing harbour basins. A free standing bottom screen of the type Silt Protector developed by the Taiyo Kogyo Corporation prevents the diffusion of the polluted bottom soil. The screen is placed in a square around the grab, see example in Figure 5.6. In deep water it can be lifted and transported easily to an other area.

Several physical model investigations have been conducted by Sawaragi at Osaka University, Japan, to study the behaviour of a screen. Flow velocities, discharges and forces have been measured. Calculation methods have been developed. In extensive field tests the aging process of the screen material have been investigated. In these tests frames with different samples have been placed in different environments, such as sea water polluted by different kinds of industrial waste, frozen water in winter and non-polluted sea water.

Most applications of Silt protector screens are floating surface screens. But bottom screens have been used also. In deep water they have been applied in combination with surface screens. A special sink-and-float type has been developed to allow ships to pass the screen freely. The screen is lowered by deflating air and raised by pumping extra air in the floats of some screen sections. These screens have been designed using a high safety factor. In general they are used succesfully for temporary work, e.g. dredging work in harbors and coastal areas in Japan.

References:

Taiyo Kogyo Corporation, leaflet: Design of Silt Protector(--)

Sawaragi, T., S.I. Aoki, H. Liu, Wave-induced impulsive forces in tension cables of a flaoting silt curtain, Proceedings of the Second International Offshore and Polar Engineering Conference, San Francisco, USA, 14-19 June 1992, pp 339 -346

Sawaragi, T. Coastal engineering- waves, beaches, wave-structure interaction,Elsevier, 1995, pp 259 and further.

Sawaragi,T., S. Aoki, A.Yasui, Tensions on silt curtains in currents and waves, Eight International Conference on Offshore Mechanics and Arctic Engineering, The Hague, 19-23 March 1989, pp 13 - 21

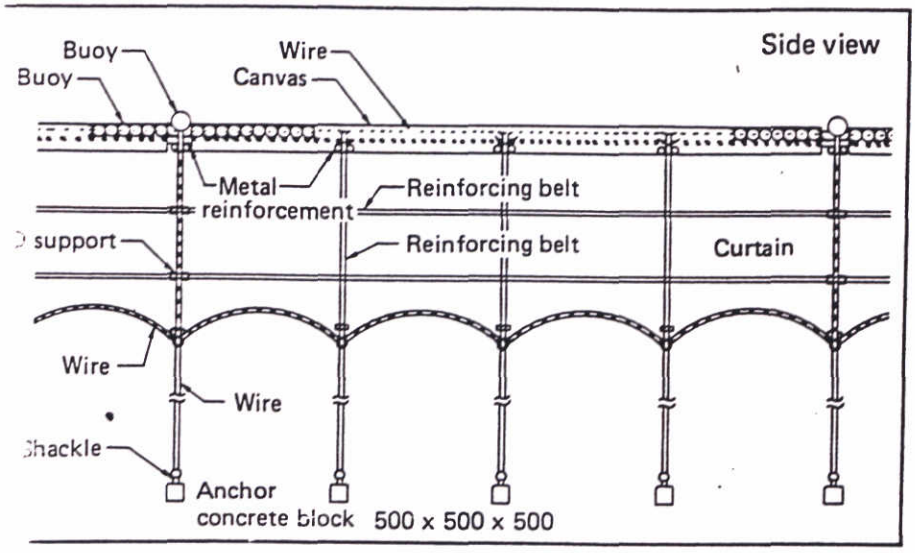

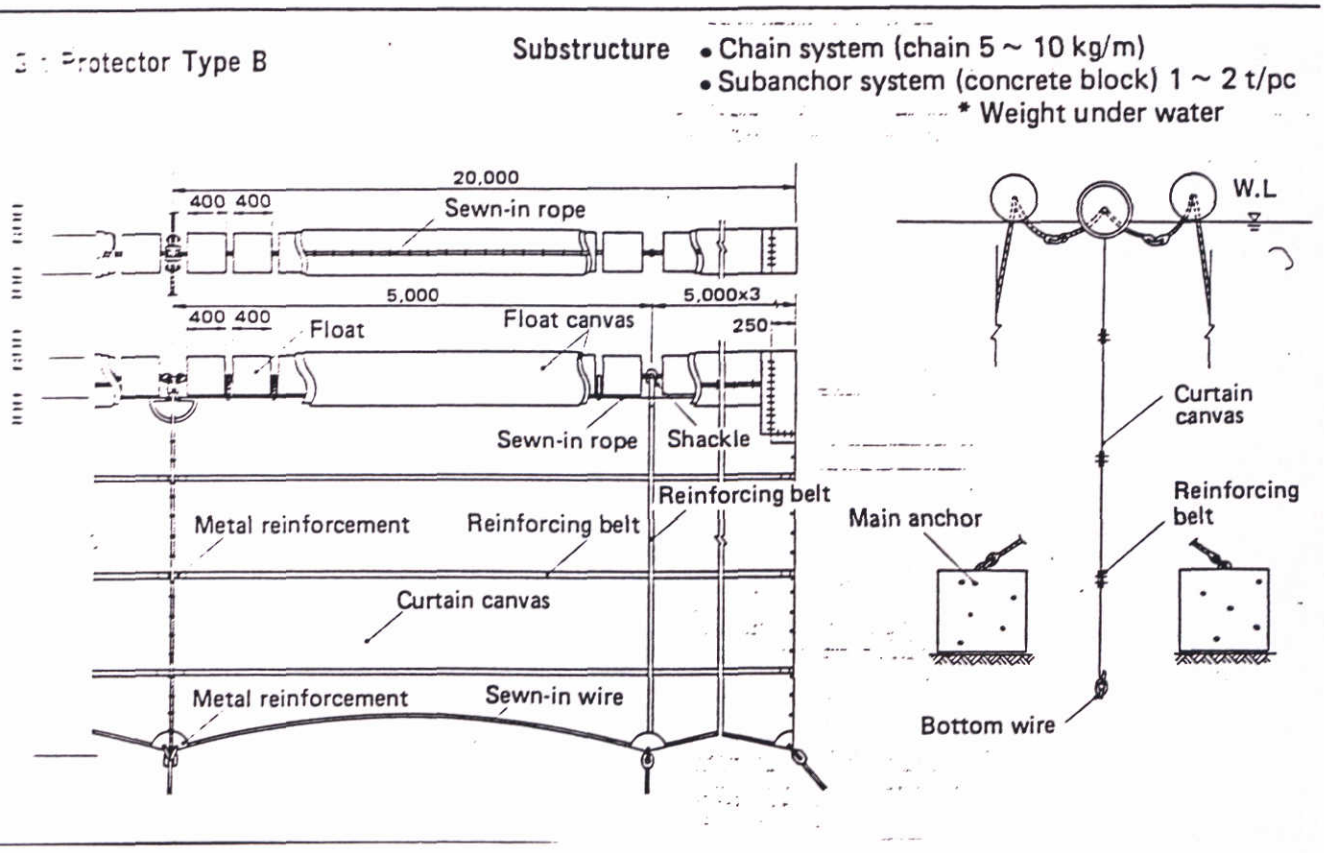

Figure 5.6 Example Silt Protector screen

5.2.4.5 Berosin cloths

A field test with Berosin cloths had been designed by Rijkswaterstaat to stop continuous beach erosion along the island Vlieland, especially around the head of a groyne. Three Berosin cloths of 25 * 25 m^2 had been placed near the head of that groyne around the low water level. These cloths have been kept in place by anchors which anchor plates had been injected by a specialized diver.
Berosin (Better Erosion Prohibiter), developed by Buro van der Hidde, are cloths of a polyethene fabric with a weight of 200 grammes per square meter anchored to the sea bed at three sides and at one side small floats have been attached to keep the cloth a few meters above the sea bed, see Figure 5.7. Part of the sediment transported by the tidel motion will deposit under, op top and around a cloth. A cloth prevents that the deposited sediments are eroded again. After some time a cloth will become less permeable by the growth of marine vegetation.

After the start of the test in May 1992 Rijkswaterstaat made weekly observations of the morphological developments around the cloths and of the cloths themselves, until October 1994. The main results are:

- Morphological developments:
  - after 3 weeks: one cloth completely filled with a 0.5 m thick sand layer, other cloths remain empty and the beach had been eroded over a length of a few hunderd meters in the area of the cloths, the three cloths have been filled 0, 100 and 0 %
  - after 10 weeks: the three cloths have been filled 50, 75 and 0 %.
  - after 20 weeks: the three cloths have been filled 90, 90 and 0 %
  - after 30 weeks: the three cloths have been filled 90, 80 and 80 %

After 30 weeks the cloths remain filled with 0.5 m thick layer of sand during the next year. After a storm in February 1993 the cloths were full with sand and the beach had been sedimented. These cloths had most probably prevented erosion of the head of the groyne, because the head of a neighbouring groyne head had been eroded about 10 m.

- Behaviour of the cloths:
  - after 9 weeks: three anchors became loose,
  - after 18 weeks: vegetation started to grow on the cloths,
  - after 39 weeks: one cloth damaged by ice, and in the following weeks the upper part of this cloth had been teared apart because of 'abrasion' of the cloth by stones which are part of the protection layer of the groyne.
  - after 60 weeks: the connections between cloth and anchor showed some damage.

The overall conlusion is that this test had shown that the Berosin cloths can prevent erosion and induce sedimentation of a 0.5 m thick layer of sand for a period as long as the cloths are in position. Vegetation on the cloths prevents erosion of this layer.
If these cloths are applied in the vicinity of protection works made of stones than it is recommended to use a heavy quality cloth, which can resist 'abrasion'. The applied cloth material is succesful on a sandy sea bed without sharp stones. Further it is recommended to use stronger connections between cloth and anchors.

References:

Bureau van der Hidde, Berosin curtains, commercial brochure

Nieuw type zinkstuk ontwikkeld voor kustvakken, rivieroevers en voor pipelines, article in OTAR, 11 pp 357 (1992),

Bouman,E., (May 1994), Evaluatie proef "Berosin" bodembescherming op Vlieland, Rijkswaterstaat

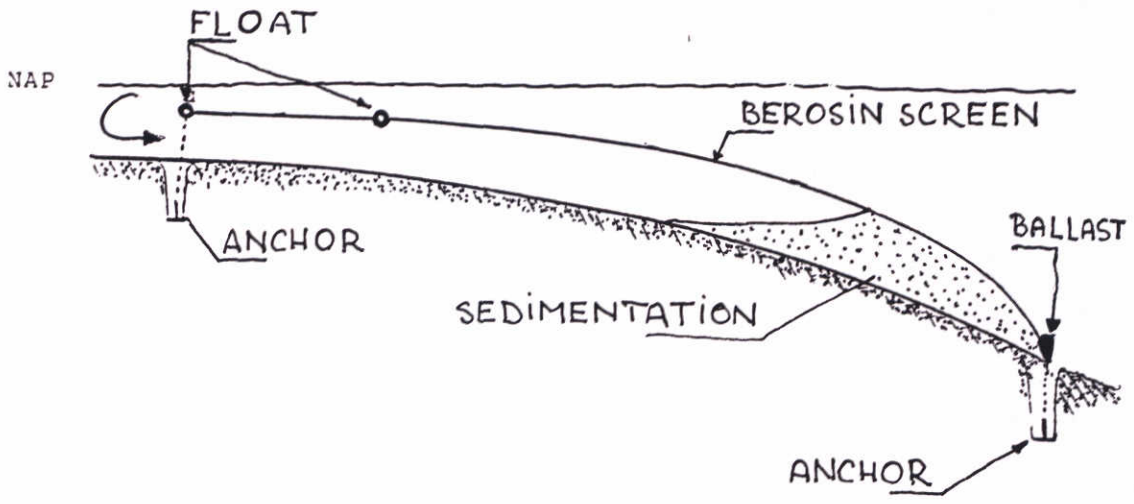

Figure 5.7 Berosin cloths

5.2.4.6 Bottom screens in Meghna river

In a test it was tried to reduce the bank erosion in the mouth of the Meghna River in Bangladesh. After consultation of several experts DHV designed a bottom screen with a ballast tube and three floating polyester tubes sewn in the fabric. Three test sections had been installed in 1997 and kept in place by anchors made of concrete blocks. A procedure to install a screen had been developed and improved using field experiences.

The three test sections have provided valuable experience to install such a screen in about 10 m deep, tidal water and to monitor the behaviour of such a system. After a short time some sedimentation had been observed around the test sections but then it became apart at the seams of the geotextile and these pilot screens have been lost. The tests will be continued with improved bottom screens.

References:

verbal communication with DHV partner in project Meghna Estuaries Studies,

5.2.4.7 Summary

The experiences with pilot projects to test bottom screens have been described in the previous sections and they are summarized in this section. A common experience is that in all field tests some damages occurred to a screen or the screen did not function as expected. In most cases the size of the damages could probably have been reduced if the application would have been developed in more small steps. A longer development process would often have resulted in a better screen designed for the local conditions. This shows that the development of a new application of a synthetic screen as a bottom screen should be planned carefully.

Some suggestions for a phased development process are the following:

- An inventory of all the forces exerted on a screen by means of field measurements and literature survey,
- A conceptual design of a screen,
- Determination of different failure mechanisms,
- Determination of the design conditions following a probabilistic approach, with the results of:
  physical model investigations,
  mathematical model simulations of flow and wave patterns and
  calculation methods to extrapolate the field measurements to design conditions,
  knowledge on the behaviour of synthetic material (aging, fatique) in the field is often insuffient and intensive cooperation with the company which produces the selected synthetic material is necessary.
- Often samples of the material and of the joints should be tested at the location of the future bottom screen.
- A small scale field test with only a few sections of the proposed bottom screen should be used to verify the results of physical model investigations and mathematical model simulations. The planning should be flexible to repeat this small scale test with a modified design.
- A detailed monitoring programme should be setup to monitor these few screen sections. The results should be analyzed together with the producer of the selected synthetic material(s).
- Final design of a complete bottom screen.
- After installation of the screen a monitoring programme should start to provide field data for an evaluation of the behaviour of a bottom screen.

Such development processes need cooperation between many participants: producer of synthetic materials, water management authority, field survey companies, consulting engineers, universities and institutes for applied research. Preferrably these development processes should be part of research and development programmes on a national or an international level.

All these steps will result in relatively high development costs, but the costs of the construction and operation of a well designed bottom screen of synthetic material will be low compared with traditional solutions. Low-budget development projects can result in disappointments and they can delay the introduction of new applications of bottom screens.

5.3 References bottom screens

Bureau van der Hidde, Berosin curtains, commercial brochure

Delft Hydraulics, Vermindering slibbezwaar Botlekhaven, R2004, Juni 1984

Gemeentewerken Rotterdam, Ingenieursbureau Havenwerken, De ontwerp-sterkte berekening van het slibscherm, 69.30-R8004, April 1980

Gemeentewerken Rotterdam, Ingenieursbureau Havens, slibscherm, deel 4, Onderzoekconstructiemogelijkheden dicht slibscherm, 69.30-R7801, Oktober 1978

Hoedt, G. den, H.E. Metz, M. Veltman, W.Voskamp, Cost-effective reduction of sedimentation and maintenance dredging using geotextile flow diversion screens, Second International Conference on Coastal and port Engineering in Developing Countries, 1987

Huygens, M., R.Verhoeven, D.de Wachter (Februari 1994)
Hydraulische modelstudie van werking en gedrag van onderwaterschermen "GESEP", Universiteit van Gent, Laboratorium voor Hydraulica, Deel A en deel B.

Huygens,M., R.Verhoeven, D.de Wachter, J.Himpe, S.Buyck, F.Wens, B de Putter and P. de Wolf, Model simulation of the impact of underwater screens on shore protection, PIANC Bulletin No 86 pp 32 - 39, (1995)

Kano, T., H.Minami and H.Kawamoto, Hydraulic model studies on effective installation method of Silt Protector sheets for large depth of working site, Coastal zone, 1989, pp 2256 - 2270

Nieuw type zinkstuk ontwikkeld voor kustvakken, rivieroevers en voor pipelines, article in OTAR, 11 pp 357 (1992),

Rijkswaterstaat, E. Bouman, Evaluatie proef "Berosin" bodembescherming op Vlieland, (mei 1994)

Sawaragi, T., S.I. Aoki, H. Liu, Wave-induced impulsive forces in tension cables of a flaoting silt curtain, Proceedings of the Second International Offshore and Polar Engineering Conference, San Francisco, USA, 14-19 June 1992, pp 339 -346

Sawaragi, T. Coastal engineering- waves, beaches, wave-structure interaction,Elsevier, 1995, pp 259 and further.

Sawaragi,T., S. Aoki, A.Yasui, Tensions on silt curtains in currents and waves, Eight International Conference on Offshore Mechanics and Arctic Engineering, The Hague, 19-23 March 1989

Taiyo Kogyo Corporation (1994), leaflet: Design of Silt Protector, Japan

6 Inflatable dams

A special group of geo-systems are inflatable dams, which are used for river regulation, flood protection, irrigation and increase of reservoir capacity. In future inflatble dams will be used as submerged breakwater near harbour entrances. Most often inflatable dams are used for water regulation as part of a water management scheme or an irrigation project. In a few cases these dams function for flood protection. The first inflatable dams were constructed about 30 years ago.

The principle of an inflatable dam is a cylinder filled with water, air or a combination of both. This cylinder, which is made of a synthetic membrane, is connected to the foundation over the whole length of this cylinder. The impounding height can be varied by in- or decreasing the internal pressure by pumps. After use the deflated membrane can be stored in the foundation of the dam and the river discharge can pass the dam without backwater effects and also navigation can pass without hindrance. Water is used most often to inflate the dam, but in some cases air or partly water and partly air have been used. The following advantages and disadvantages should be considered for the selection of water or air: a cylinder filled with water has a lower impounding height as a cylinder filled with if the circumference of the cylinder is the same. But an air filled cylinder induces higher forces on the foundation and often their dynamic response to wave loading induces higher forces in the cylinder than a water filled cylinder. An air filled cylinder can be entered for inspection and maintenace and this is not possible with a water filled cylinder.

Simulations with mathematical models or testing in physical models are standard tools for the design of an inflatable dam. Two and three dimensional mathematical models are under development and these models are often used for a preliminary design. Two dimensional models often consider a cross-section of the cylinder. To design the connection of the cylinder to the bank a three dimensional model might be necessary. For a final design the dynamic response of the cylinder to irregular wave loading, the storage of the cylinder in the foundation while deflating the cylinder and the vibration forces in the cylinder by overflowing water are often measured in a physical model. The elastic properties of the synthetic material of the cylinder has to be reproduced in the model on scale. Thedesign process might include field testing of samples of different synthetic materials and testing of end sections on prototype scale (1:5 to 1:1).

Several aspects relevant for the design and the operation of such dams have been described in Section 6.1 with emphasis on the properties of the available materials for the membranes of these dams. An outlook on the calculation methods for the forces in and the shape of the membrane is presented in Section 6.2.

The definition of the main parameters of an inflatable dam are, see Figure 6.1:

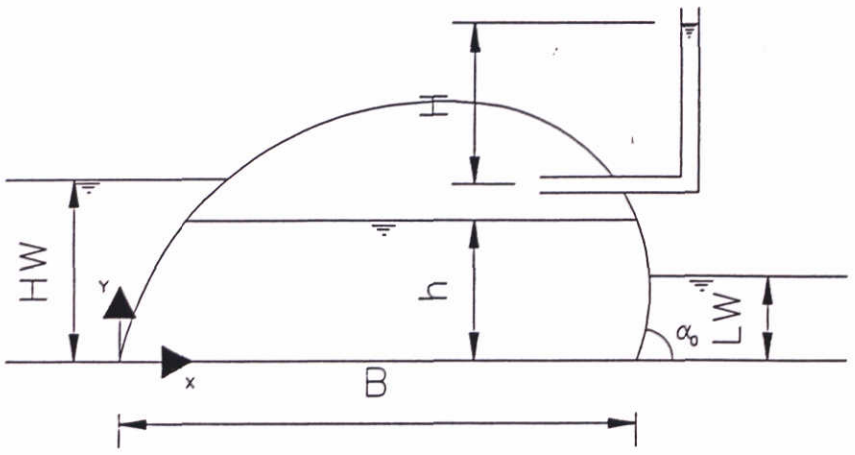

Fig. 6.1 Main parameters of an inflatable dam

Ψ = angle with the horizontal (= positive x-axis)
B = width of the cylinder at the foundation (m)
y_1 = pressure in the cylinder at the bottom (m water column)
L = length of the circumference of the cylinder (m)

Design parameters are the tension force in the membrane, T (N) and the impounding height or the difference between the high water level and the lower water level.

The relevant properties of the membrane are its thickness, density or weight per square meter, elasticity, strength, and elongation at failure.

6.1 Constructional aspects

The main part of an inflatable dam is an inflatable synthetic membrane which is connected with a foundation and side walls. In general the deflated membrane is stored in or on a foundation. A pumping system inflates the dam with air or water. Most dams use water to inflate the dam. In general these dams are weirs with a height of 1 to 2 m. The impounding water height of existing dams is maximum 6 m. The length of a dam varies of several meters in small canals (often used for irrigation) to about 50 m in rivers. The new dam planned for Ramspol will have an impounding height of 9 m and it will be one the biggest inflatable dams in the world. The expected life time of membrane dam varies between 15 and 30 years. The costs of construction and maintenance are relatively low compared with traditionally designed dams. A few companies are specialized in the construction of inflatable dams, for example Kloeckmuhle and Vreedestein in Europe, Goodrich in USA and Bridgestone and Sumitomo in Japan. The addresses of these companies are:

Bridgestone Tyre Corporation
Planning Department Rubberdam Group
Chemical and Industrial Goods Division
No 1-10 Kyobashi 1-chome, Chuo-ku, Tokyo 104, tel. 03 567 0111
London Office, West End House, 11 Hills Place, London W1R 1AG, tel. 01 734 2804

Floecksmuhle Energietechnik GmbH
Bachstrasse 62-64
5100 Aachen, tel. + 49 241 531175

Sumitomo Electric Industries LTD
Tokyo Sales Department
3-12 Moto-Akasaka 1-chome, Minato-ku, Tokyo 107, tel. 03 423 5151

Rubberfabriek Vredestein Loosduinen NV
no address, Vredestein Dilataties Renkum tel 0317 399272 might provide additional information

A membrane often exists of a synthetic fabric with a coating on both sides. A coating makes a synthetic fabric water tight and improves the chemical properties of a membrane. Synthetic materials are for example polyester (PET), polyamide (PA, nylon), polypropene (PP), neoprene, aramide (Kevlar and Twaron) and polyethene (Dyneema). The main properties of these materials are presented in Table 6.1. A membrane can also be made of a natural material, for example rubber. For small dams Bridgestone (1987) has applied membranes of Ethylene Propylene Diene Monomere (Dyneema) successfully.

The strength at failure of synthetic materials reduces in time and this process is called aging. In general no sufficient data on the effect of aging is available, because many different synthetic materials exist and an aging process depends on the environment of the material. For example the reduction of the permissible strength in time is different in sea water and in fresh water, see the tests done by Taiyo Kogyo Corporation (1994). Often high safety factors have to be selected to include the effect of aging in the design. Taiyo Kogyo Corporation proposed a safety factor 10 to 20 for semi-permanent surface and bottom screens in sea water. Dutch Rijkswaterstaat proposed a safety factor of 4 in weft direction and 6 in warp direction of a woven polyester fabric for an inflatable dam in a fresh water environment. Floecksmuhle (Dumont, 1988) recommended a safety factor 10 for small inflatable weirs in rivers.

Synthetic material	*Density*	*Strength*	*Modulus*	*Elongation at failure*	*Sensitivity for fatigue *)*
Unit	kg/m^3	10^9 N/m^2	10^9 N/m^2	%	-
PET	1380	1.1	14	13	-
PolyPropylene	900	0.6	6	20	+
Poly Amide 6	1140	0.9	6	20	-
Aramide	1440	2.8	75	3.7	++
Dyneema SK60	970	2.7	87 - 89	3.5 - 5	-
EPDM	?	0.17	0.48	?	?

*) + = sensitive, - = not sensitive

Table 6.1 Properties of different materials for fabrics (TNO, 1997, Bridgestone,1987)

Coatings can be made of polyethene, polyurethane and softened PVC-P. Other properties as aging, fatigue, tear-strength, and influence of low temperatures on the material properties are important for the selection of materials. Often not sufficient data are available, especially on aging and fatigue of materials.

For dams in urban areas it is recommended to add a special reinforced membrane with a mailed layer of a special woven metal wire to resist vandalism (TNO Industrie, 1997).

Joints of the membrane should be as strong as the membrane itself. In some cases this required a special laser-technique and a sufficient width of the overlap.
It is recommended to test sample joints.

The width of the foundation is determined by the required space for the pipes to fill and to empty the dam and the minimum required width for the stability of the foundation. The membrane is anchored to the foundation. The width between the upstream and the downstream anchorage is a design parameter.

To connect a membrane with the foundation it is clasped or clenched with bolts and nuts to a steel frame. The aging process of synthetic materials can result in a reduction of the clasping force over time. In the design this connection should get proper attention.

The storage process during deflation of the membrane can be complicated if the flow changes its direction (for example in estuaries).

In rivers possible sedimentation on a deflated dam needs proper attention. If river water is used to inflate the dam suspended material can settle inside the membrane and form a layer of fine silt and clay after a long period.

If the dam functions as a weir than a so-called V-notch effect has been observed frequently (Ogihara, 1984). Locally the flow over the dam concentrates and lowers the dam in the shape of a V-notch. The location of this V-notch effect over the dam varies and is unpredictable. This effect may require reinforcement of the downstream bed protection.

6.2 Calculation method

6.2.1 Introduction

In general simple calculation methods of the forces and the deformations of an inflatable dam are based on a differential equation for a 2-D cross-section of an inflatable dam.

The shape of the membrane of an inflatable dam is described by a second order differential equation, see van der Burg (1961), Pover (1993), Dorreman (1997) and Parbery (1978). In general the water levels are different at both sides of the dam:

$$T\frac{d\psi}{ds} = \frac{T\frac{d^2y}{dx^2}}{\left(1+\left(\frac{dy}{dx}\right)^2\right)^{3/2}} = -\rho\, g\, y_1 \qquad (115)$$

in which
T tension force in membrane (N/m')
Ψ angle with horizontal (degrees)
s length of membrane (m)
y_1 measure for the internal pressure (vertical height)
g acceleration by gravity (m/s2)
ρ density of water (kg/m3).

The own weight of the membrane and the elongation of the membrane are neglected in this equation. Calculations have shown that in general the influence of the weight of the membrane on the shape of the membrane is very small in water filled dams. However, the elongation of the membrane can be considerable and it has some influence on the shape of the membrane, especially on the height of the dam. It can be included by replacing ds by ds + ds' in which ds' is the elongation because of T, see Parbery (1967) and Dorreman (1997).

Inflatable dam	y_1
water filled dam which is completely under water (van den Burg)	$(H - h_u)$
water filled dam partly above water (van den Burg)	$(H - y_1)$
air filled dam (Parbery)	(H)

Table 6.2 Different expressions for the pressure in the dam.

In airfilled dams the internal pressure is constant and in water filled dams the internal pressure reduces with the distance above the bottom of the dam, see Table 6.2.

Formula (115) shows some similarity with the differential equation for surface and bottom screens as described in the previous chapters. In addition to this equation the overall horizontal and vertical equilibrium of the forces can be checked.

6.2.2 Analytical solutions

The most important parameters for the design of a dam are the tension in the membrane T and the height of the crest of the inflated dam. For the case of an inflated dam, loaded by hydrostatic pressure only analytical solutions have been derived by many authors, for example van den Burg (1961), Parbery (1967), Plaut (1997) and Watson (1985).
Watson (1985) presented a derivation of the formulas for the shape of an inflatable dam. He defined dimensionless axis as:

$$\xi = \frac{x}{y_1} \qquad (116)$$

and

$$\eta = \frac{y}{y_1} \qquad (117)$$

in which y_1 = the internal pressure at the bottom expressed in meters water column. In the calculation of the shape of the dam y_1 is often treated as a constant.

The shape of the membrane is described by:

$$\xi = -(1 - \frac{1}{2} k^2)\, F(\phi,k) + E(\phi,k) \qquad (118)$$

$$\eta = \pm\sqrt{1 - k^2 \sin^2\phi} \tag{119}$$

in which:

$$k^2 = \frac{4\,T}{\rho\, g\, y_1^2} \tag{120}$$

k = modulus of elliptic functions
$F(\phi,k)$ = Legendre's form for the elliptic integral of the first kind
$E(\phi,k)$ = Legendre's form for the elliptic integral of the second kind

$$F(k,\phi) = \int_0^{\phi} \frac{d\theta}{\sqrt{1 - k^2 \sin^2\theta}} \tag{121}$$

$$E(k,\phi) = \int_0^{\phi} \sqrt{(1 - k^2 \sin^2\theta)}\, d\theta \tag{122}$$

The value of $F(\phi,k)$ and $E(\phi,k)$ can be determined by expansions of these elliptic functions or to use tables with these functions (Abramowitz and Stegun, 1965). An example of the use of expansions has been shown by Namias (1985), mentioned by Plaut (1997) for k^2 if k is not extremely close to unity. In that case k is a function of the perimeter of the dam and the internal pressure (m water column) and it does not depend on tension T:

$$k^2 \approx \frac{2\,L}{\pi y_1} - \frac{3\,L^2}{2\,\pi^2\, y_1^2} + \frac{3\,L^3}{8\,\pi^3\, y_1^3} \tag{123}$$

in which L = perimeter of the dam (m)
These formulas describe two types of inflated dams depending on the value of k:
water inflated dams: $k <= 1$, the shape of the dam from $\phi = 0$ to $\phi = \pi$,
crest at $\phi = \pi/2$, see Figure 6.2, and
air inflated dams: $k > 1$, the shape of the dam from $\phi = 0$ to $\phi = 2\pi$,
crest at $\phi = \pi$ and
the points of inflection occur at $\phi = \pi/2$ and $\phi = 3\pi/2$, see Figure 6.3.
According to Watson ϕ has no obvious physical significance, at the best relation between ϕ and the angle ψ between the membrane and the horizontal appears to be:

$$\cos\psi = 1 - 2k^2 \sin^2\phi \tag{124}$$

The two unknowns y_1 and the angle Ψ between the bed and the membrane at the anchorage can be determined from two equations for the length of the membrane and the distance between the anchorages at the bed.

If T is given the height of the dam and its shape can be determined with the given formulas. Or if the internal pressure is given, than k can be estimated with an approximative formula, next T can be estimated with the definition of k and the height of the dam can be determined by (118) and (119). Some examples are presented in Figure 6.4 for an air inflated dam and Figure 6.5 shows different stages of a water inflated dam.

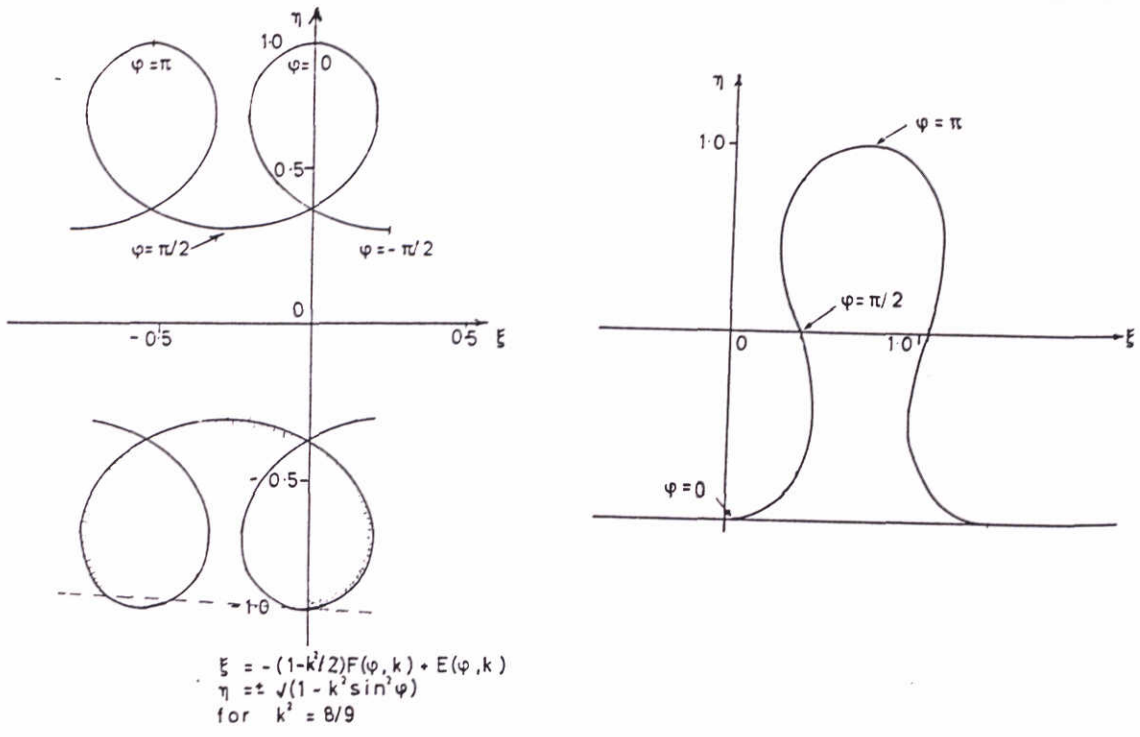

Figures 6.2 and 6.3 Shape on the membrane of a water filled dam and an air filled dam according to Watson (1985)

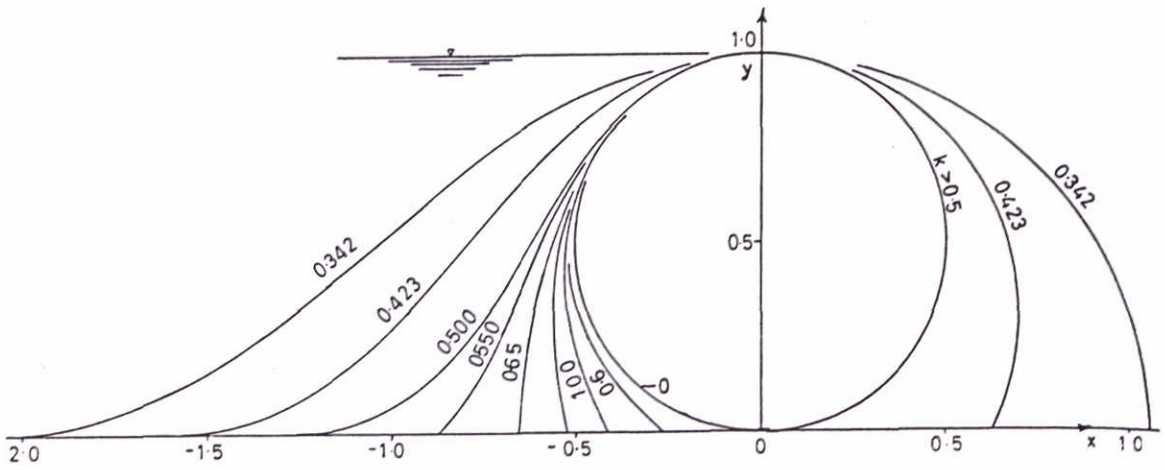

Figure 6.4 Air inflated dams for various k and constant height of the dam (according to Watson 1985)

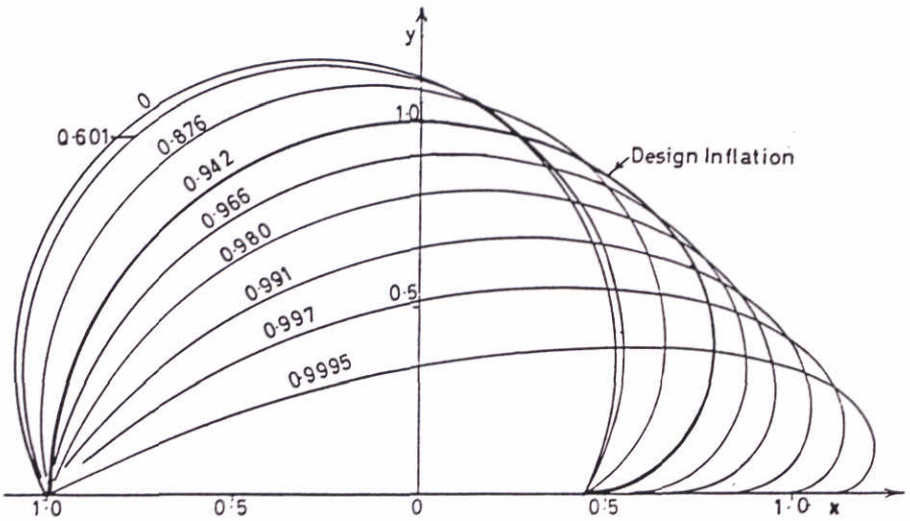

Figure 6.5 Different stages of water filled dam, values of k shown (according to Watson 1985)

For geotubes (sausages) Plaut (1997) presented some analytical solutions. He defined a dimensionless axis by x/L and y/L where L = length of the membrane (m) and his analysis resulted in the same expressions for ζ and η as (118) and (119), see Figure 6.6.
The height of a water inflated geotube laying in the air on a rigid horizontal foundation:

$$h = (1 - \sqrt{1 - k^2})\, y_1 \qquad (125)$$

in which
y_1 = internal pressure (meters water column)
h = height of a water inflated geotube (m)
k = modulus of elliptic functions

This formula can also be applied to completely submerged geotubes.
In case an inflated dam is loaded by waves no analytical solutions for the vibrations and the dynamic forces in the membrane have been found in the available literature.

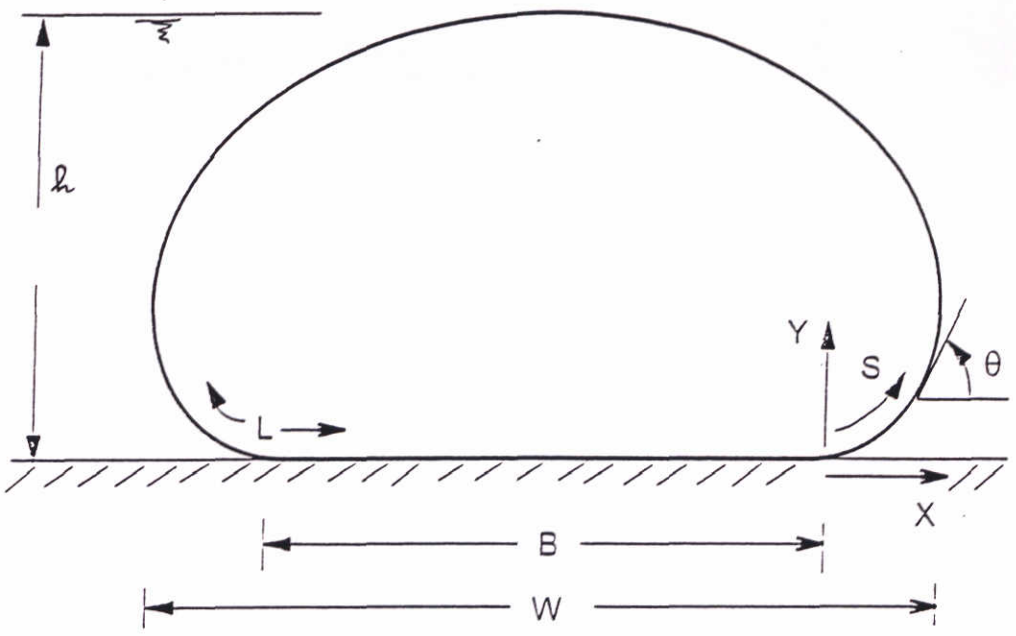

Figure 6.6 A geotube on a rigid foundation according to Plaut (1997)

6.3.3 Numerical solutions

Various numerical models have been developed for a hydrostatically loaded dam inflated with water, for example by Rijkswaterstaat, Pover (June 1993) and Dorreman (1997). Dorreman (1997) made a spreadsheet model for a dam loaded by hydrostatic forces only. The model has been based on the formulas publiced by van den Burg (1961), Parbery (1976, 1978) and Harrison (1970). The calculation starts in an anchorage point and proceeds along the segments of the membrane. At the end of the calculation it is checked if the end point is in the position of the other anchorage point. If not, the calculation has to be repeated with adjusted segments. This model calculates the shape of the membrane and the forces in the membrane. These results have been confirmed by the results of physical model investigations.
However, in practice infaltable dams are often also loaded by waves and the dynamic response of the dam to wave loading determines often the design. The numerical model developed by Pover can be extended to include also the dynamic response due to wave loading. A model to estimate the dynamic response of n inflatable dam to wave loading has been prepared by WL, van Meerendonk (June 1996). This model is based on a strong schematization of the relevant phenomena. If a dam is used as a weir than oscillations of the membrane can be caused by instabilities in the overflow and in the downstream recirculation (Hitch, 1984).

For the design is the dynamic response of a dam during the filling stage and in the operational stage most important.

Pover had made a spreadsheet model which solves the second order differential equation with the corrector -predictor method according to Euler and Heun. The force equilibrium on a small segment of the membrane is considered. A consequence is that the membrane has to be divided in segments where different forces are active: downstream under water, downstream above water, upstream under water and upstream above water. The number and the length of the segments of the membrane are input parameters. After the calculation the assumed length of the perimeter is checked with the results of the calculation. In practice this is a limitation of the calculation method. The user selects the maximum force in the

membrane T and the length of the membrane. The model calculates the maximum height of the dam. The results of the model have been confirmed with the results of physical model investigations.

Next Pover had developed a finite-element model with the software package ANSYS to calculate the forces, the elongation and the deformation of the membrane under hydrostatic load. Also the results of this model have been confirmed with the results of physical model investigations.

Van Meerendonk (1996) considered a 2-dimensional cross-section of the dam which has been schematized as a non-linear mass-spring system with free movements in horizontal direction. The input of the model are irregular waves and the model calculates the shape of the mebrane and the forces in the membrane. The solved equation of motion is:

$$F(t) = m\,\ddot{x}(t) + c\,\dot{x}(t) + k(x)\,x(t) \qquad (126)$$

in which

F(t)	=	external force in x-direction as function of time t (N)
m	=	moving mass = mass of the dam + added mass (kg)
c	=	damping (Ns/m)
k	=	spring characteristic (N/m)
x(t)	=	position of the centre point of the moving mass at time t relative to the initial position

The added mass and added damping have been calibrated on the results of physical model investigations. Added mass m' is calculated by (Berkhof, 1976) :

$$m' = c_m\,\rho\,h^2 \qquad (127)$$

in which h = water depth (m), ρ = density of water (kg/m^3) and c_m = calibrated coefficient (-).

The calculations have shown that the dam start to move when the frequency of the incoming waves is close to the resonance frequency of the dam. This resonance frequency increases if the internal pressure is increased. The resonance frequency can be changed by selecting an air or water filled dam or a dam partly filled with air and partly with water. These results can be used in a sensitivity analysis of different design parameters, because the calculation method is based on several assumptions and therefore the accuracy of the results is not high.

6.4 References inflatable dams

Abramowitz, M. and I.A. Stegun, (1965), Handbook of mathematical functions with formulas, graphs and mathematical tables, Dover, New York, USA

Bridgestone Tire Co. Ltd., (1987), Study and countermeasures for vandalism on rubber dam, marine and Industrial news, No 2, pp 2-8

Burg, H.J. van der, (December 1961) De berekening van een stuw van rubber, De Ingenieur, bouw en waterbouwkunde, pp 229 - 235

Berkhoff, J.C.W., (1976), Trillingen sluisdeuren, verslag wiskundig onderzoek W254, Delft Hydraulics,

Dorreman,J.,(May 1997), Technical University Delft, Civil engineering, Bagstuwen gevuld met lucht en/of water (Dutch)

Dumont U., (1988) Schlauchwehre-Technik, Funktion und Einsatz, Wasserwirtschaft, Vol. 78, Issue 7/8, Pp. 311, 314-316

Harrison, H.B. (April 1970) The analysis and behaviour of inflatable membrane dams under static loading, Proceedings of the Institution of Civil Engineers, Vol. 45

Hitch, N.M. and Narayanan, R., (April 1984), Pressure field over rigid model of an inflatable dam, Channels and channel control structures, Proc. 1st Int. Conf. Hydraulic Design in Water Resources Eng., University Southampton, Berlin, Springer-Verlag, pp. 1-(119-131)

Langeveld, P.C.G., (June 1997) Haalbaarheidsonderzoek balgkering Kampen, TNO Industrie (in Dutch)

Meerendonk, E. van (June 1996), Balgstuw Ramspol, Literatuuronderzoek en rekenkundig onderzoek, Delft Hydraulics, (in Dutch)

Ogihara, K. and H. Saito, (September 1984), Rubber dam, Proceedings Fourth congress Asian and Pacific Division of International Association of Hydraulic Research, Chiang Mai, Vol. I, pp 593-602

Parbery, R.D., (December 1976) A continuous method of analysis for the inflatable dam, Proceedings of the Institution of Civil Engineers, Vol. 61, part 2

Parbery, R.D. (September 1978) Factors affecting the membrane dam inflated by air pressure, Proceedings of the Institution of Civil Engineers, Vol. 65, part 2

Plaut, R.H. and S. Suherman, (1997), Two-dimensional analysis of geo-synthetic tubes, submitted to Journal of Geotechnical en Geo-environmental Engineering, ASCE

Pover, J.P., (June 1993) Berekening Balgstuw Ramspol, Rijkswaterstaat (in Dutch)

Taiyo Kogyo Corporation (1994) Design of Silt Protector, commercial brochure

Watson, R. (1985) A note on the shape of flexible dams, Journal of hydraulic research, Vol. 23, no 2, 179 - 194

Appendix 1 References

The following literature has been collected for this study, but not all these references have been used in this report. This literature refer not only to the application of geotextiles for the construction of inflatable dams, floating and bottom screens, but also other structures as dividing screens in reservoirs, geotubes, breakwaters, beach protection systems and others.

Abromeit, H.-U., 1996, Ship-induced geotextile tensile stresses during installation under water - theoretical assessment and verification, Proc. of the 1st European Geosynthetic Conf. Eurogeo 1, Maastricht.

AKZO, 1991, Armater and Enkamat, company publications, Arnhem, The Netherlands.

Alberts Alligator bv: Kijk op Kunststof, Product info.

Anonymous, Inflatable dams for variable central-water power and dam construction, p.49, March 1976.

Anonymous, 15 Maart 1967, Nederlands ingenieur ontwierp kunstmatige stuw, Bedrijf en Techniek, 22, no.535, p. 419.

Anonymous, December 1971, Schlauchwehre in der Schweitz, Fördern und Heben, 21, no.16, p.967.

Anonymous, Oktober 1969, Oppompbare waterkering in de Weespertrekvaart in werking gesteld, Water, 53, no.10, p.577-578.

Anonymous, November 1969, Barrage mobile - nouveau projet spectaculaire et prometteur pour dominer l'eau des fleuves, des rivières et des canaux, La Techn. de l'Eau et de l'Assainissement, no.275, p.51-54.

Anonymous, 1970, Nederlands eerste hydrostuw in werking, Water, 54, no.11, p.659.

Anonymous, mei/juni 1972, Hydro-stuw, Land en Water, 16, no.3, p.36-37.

Anonymous, ca. 1972, Inflatable barrages in practice.

Anonymous, March 1976, Inflatable dams for variable control, Water, Power and Dam Construction, p.49.

Anonymous, Hydro barrage.

Anonymous, Mai 1973, Überschwimmungsschutz durch wassergefüllte Sperrschläuche, Baumaschine und Bautechnik, 20, no.5, p.196.

Anwar, H.O., May 1967, Inflatable dams, Journal of the Hydraulics Division, ASCE, Vol.93, No.HY3, p.99-119.

Anwar, H.O., December 1975, Inflatable dams for irrigation projects, Proceedings Second World Congress, Water for Human Needs, International Water Resources Association, Vol.V, p.317-321, New Delhi.

Berkhof, J., February 1976, Trillingen sluisdeuren, W254, Delft Hydraulics

Binnie, A.M., 1973, The theory of flexible dams inflated by water pressure, Journal of Hydraulic Research 11, no.1.

Blondé, A., 1960, Nylon bij noodwaterkeringen voor stormvloeden, Techn. Wet. Tijdschrift 29, no.10, p.237-239.

Bouman, E., May 1984, Evaluatie proef "Berosin" bodembescherming op Vlieland, Rijkswaterstaat

Brian, E.W. and P.Dowse, 1979, Hydrostatically supported sand coastal structures, Coastal Structures '79, ASCE.

Bridgestone Tire Co. Ltd., 1987, Study and countermeasures for vandalism on rubber dam, marine and Industrial news, No 2, pp 2-8

Bridgestone Tire Co. Ltd., 1987, Rubber dam utilized as tidal barrier (Naruse, Japan), Commercial Brochure.

Bridgestone Tire Co. Ltd., 1983, The functions and operating installations of new rubber dam, Commercial brochure.

Bridgestone Tire Co. Ltd., 1982, Results of hydraulic experiments, Commercial Brochure.

Bridgestone Tire Co. Ltd., 1984/6, Rubber dam, Commercial Brochure.

Bridgestone Tire Co. Ltd., System for inflating and deflating the rubber dam, Commercial Brochure.

Broderick, L.L., 1991, Interaction of water waves and deformable bodies, 172p., Corvallis, Oregon State University, Thesis.

Broderick, L.L. and C.H.Jenkins, 1993: Experimental investigation of fluid-filled membrane breakwaters, J. of the Waterways, port, Coastal and Ocean Engineering, ASCE 119(6), pp.639-656.

Bureau van der Hidde, 1995: Berosin, product information, commercial brochure

Burg, H.J. van der, De berekening van een stuw van rubber, De Ingenieur, bouw en waterbouwkunde, December 1961

Chervet, A., 1984, Model-prototype comparisons of the defective behaviour of an inflatable dam, Federal Institute of Technology, Zürich, Switzerland.

Connor, L.J. and Grad, B.E., October 1969, Fabridams - Their application on flood mitigation projects in New South Wales, ANCOLD Bulletin no.29, p.56-65.

Christensen, B.S., L.Kock, 1997, Silt curtains, design criteria and practical application especially forRo-Boom silt curtans, CEDA Dredging Days, Amsterdam, 20-21 november

Deron Austin of Jessup, 1992, Steep slope protection using geocells, Geosynthetic World, April/May.

Dette, H.H. and A.J.Raudkivi, 1994, Dune protection, Intern. Symp. WAVES '94, Vancouver, Canada (see also 24th ICCE, Kobe, Japan

Dorreman,J., May 1997, Technical University Delft, Civil engineering, Bagstuwen gevuld met lucht en/of water (Dutch)

Doty, C.W., Thayer, W.B. and Jessup, R.G., June 1984, Automated fabric dam aids water research project, Int. Conf. on Geomembranes, Denver, Proc. Vol.I, p.127-132.

Dowse, B.E.W., H.G.Gilchrist and J.P.Capps, 1979, The varied uses of hydrostatically supported sand structures in offshore engineering, 1st Canadian Conf. on Marine Geotechnical Engineering, Canadian Geotechnical Society, Calgary, Canada, April 1979.

DSM, January 1995, Dyneema The top in high performance fibers, properties and applications, Brochure DSM High Performance Fibers B.V.

Droscha, H., Mai 1974, Ein Wehr ohne Aufbauten über dem Wasser, Schiff un Hafen, 26, no.5.

Dumont U., 1988, Schlauchwehre-Technik, Funktion und Einsatz, Wasserwirtschaft, Vol. 78, Issue 7/8, Pp. 311, 314-316

Dumont, U., October 1989, The use of inflatable weirs for water level regulation, Water Power and Dam Construction, Vol.41, No.10, p.44-46.

Evans, D.V. and C.M.Linton, 1991: Submerged floating breakwaters, J. of Offshore Mechanics and Arctic Engineering, 113, August, pp.205-210.

Firt, V., 1983, Statics, formfinding and dynamics of air-supported membrane structures, Uitgeverij Martinus Nijhoff, Den Haag.

Floecksmühle Energytechnik GmbH, Inflatable wiers, Commercial Brochure.

Fujisawa, M. and Graves, S. 1989, The installation and use of inflatable gates for raising the crest of dams, Conference on Civil Works, Zürich.

Galina, I.L., 1979, Flow from a channel with a flexible barrier (translated from Russian) J. Appl. Math. Mech., 43, no.1, p.96-103.

Geleedst, M., 1967, Balgstuw Berkelse Zwet, rapport modelonderzoek, M912, Waterloopkundig Laboratorium.

Gemeentwerken Rotterdam, Ingenieursbureau Havens, October 1978, Slibscherm, deel 4, Onderzoekconstructie mogelijkheden dicht slibscherm, 69.30-R7801,

Gemeentewerken Rottterdam, Ingenieursbureau Havenwerken, March 1980, Modelonderzoek t.b.v. het slibscherm, CO.69.30 - R80.02,

Gemeentewerken Rotterdam, Ingenieursbureau Havenwerken, April 1980, De ontwerp-sterkte berekening van het slibscherm, 69.30-R8004

Giesecke, J. and Horlacher, H.B., 1987, Model tests to prevent oscillations of flexible weirs, Proceedings IARH-Congress, Lausanne, p.270-271.

Giesecke, J., et al, 1985, Automatically operating flexible weirs in small hydropower stations in agric irrigation systems.

Giroud, J.P., T.Pelte and R.J.Bathurst, 1995, Uplift of geomembranees by wind, Geosynthetics International (Special Issue on Design of Geomembrane Applications) Vol.2, no.6.

Goda, Y., 1985, Random seas and design of maritime structures, University of Tokyo Press

Groen, P.van, June 1984, Vermindering slibbezwaar Botlekhaven, R2004, Delft Hydraulics

Groot, C. de, 1993: Tuindorp Oostzaan ver vooruit, TU Delft, Faculteit Civiele Techniek, afstudeerrapport.

Günther, H. und Jäger, F., 1970, Flexibeler Staukörper auf dem Muldewehr Penig, Wasserwirtschaft-Wassertechnik, 20, no.10, p.332-336.

Hafner, E., Mai 1979, Entwurf eines neuen Membranwehres, Wasser und Boden, 31, no.5, p.135-137.

Hafner, E., 1983, Schlauchwehre für kleine Wasserkraftanlagen, Wasserwirtschaft, 73, no.2, p.53-54.

Hales, L.Z., October 1981: Floating breakwaters - state-of-the-art, Chapter X: Flexible membranes, CERC, Technical report 81-1

Hallam, M.G., N.J. Heaf and L.R. Wootton, June 1977, Report UR8, Dynamics of marine structures: methods of calculating the dynamic response of fixed structures subject to wave and current action, CIRIA Under Water Engineering Group, London

Harrison, H.B., April 1970, The analysis and behaviour of inflatable membrane dams under static loading,Proceedings of the Institution of Civil Engineers, Vol. 45

Harrison, H.B., 1976, Interactive nonlinear structural analysis, Proc. ASCE, J. Structural Div., 102, ST7, p.1353-1364.

Herpen, J.A. van, 1996: Three dimensional synthetic mats in dike and bank protection, Proc. of the 1st European Geosynthetic Conf. Eurogeo 1, Maastricht (also: Simplified design ENKAMAT, AKZO NOBEL, Arnhem).

Hitch, N.M. and Narayanan, R., July 1983, Flexible dams inflated by water, Journal of Hydraulic Engineering, Vol.109, No. 7, p.1044-1048.

Hitch, N.M. and Narayanan, R., April 1984, Pressure field over rigid model of an inflatable dam, Channels and channel control structures, Proc. 1st Int. Conf. Hydraulic Design in Water Resources Eng., University Southampton, Berlin, Springer-Verlag, pp. 1-(119-131)

Hoedt, G. den, H.E.Metz, M.Veltman, and W.Voskamp, 1987: Cost-effective reduction of sedimentation and maintenance dredging using geotextile flow diversion screens, 2nd Int.Conf. on Coastal and Port Engineering in Developing Countries, Vol.II, Beijing, China.

Hshieh, J.C., 1988, Free vibration of inflatable dams, M.Sc. dissertation, Virginia Polytechnic Institute and State University.

Huis in 't Veld et al, 1987, The Closure of tidal basins, Delft University Press, Delft

Huygens, M., R.Verhoeven, D.de Wachter, Februari 1994, Hydraulische modelstudie van werking en gedrag van onderwaterschermen "GESEP", Universiteit van Gent, Laboratorium voor Hydraulica, Deel A en deel B.

Huygens, M., D.de Wachter, R.Verhoeven, J.Himpe, S.Buyck, F.Wens, 1994: Underwater screens for shore protection, Symp.Waves, Vancouver, Canada.

Huygens, M., R.Verhoeven, D.de Wachter, J.Himpe, S.Buyck, F.Wens, B de Putter and P. de Wolf, 1995, Model simulation of the impact of underwater screens on shore protection, PIANC Bulletin No 86 pp 32 - 39

Huijsmans, L., 1988: Ontwikkeling van een onderwaterspuitdam te Flaauwe Werk, Katholieke Industriële Hogeschool DE NAYER (zie ook meetverslag DWW 1989).

Kano, T., H.Minami and H.Kawamoto, 1989, Hydraulic model studies on effective installation method of Silt Protector sheets for large depth of working site, Coastal zone, pp 2256 - 2270

Karelse, M., 1996: Een flexibel separatieschermin een drinkwaterbekken, TU Delft, Faculteit der Civiele Techniek, afstudeerscriptie (incl.pc-model).

Kato, M. and K.Hamanaka, 1993: Analytical and experimental study of characteristics of textile sheets structures, 11th Australasian Conf. on Coastal and Ocean Engineering, Townsville, Australia.

Kim, M.H. and S.T.Lee, 1996: Flexible membrane wave barrier. I: Analytical and numerical solutions, J.of waterways, Port, Coastal and Ocean Engineering, Vol.122(1).

Kooman C., A. Hoekstra (1969) Afsluiting Volkerak, Deel IV Wind en stroom weerstand caisson en Deel V Krachten door de stroom op caissons tijdens plaatsings manouvres, M878, Delft Hydraulics

Langeveld, P.C.G. (June 1997) Haalbaarheidsonderzoek balgkering Kampen (Dutch), TNO Industrie

Lee, J.F. and C.J.Chen, 19??: Wave interaction with hinged flexible breakwater, J. of Hydraulic Research 28(3), pp.283-295.

Legisa, D., 1979/1980 Hydraulic model study of an inflatable weir, Porocilo O Strokovnem Delu, Ljubljana, p.20-22, Vognogospodarski Inst.

Lievense, J., 17 augustus 1964, Oppompbare bodemslab voor het keren van water, Octrooiraad-Nederland, aanvrage no.276301.

Looff, A.P. en P.Roelse, 1996: BEROSIN - evaluatie proefprojecten en mogelijke verdere toepassingen van deze vorm van kustverdediging, RWS, rapport DWW-96-074/RIKZ/AB-96.847X, Juli.

Maurer, J., 1972, Elastische Schlauchwehre, Wasserwirtschaft 62-11, p.346-350.

Marshall, December 1974, Rubber dams proposed to end Venice floodperil, Rubber World no.3, p. 56-59.

Meerendonk, E. (June 1996) Balgstuw Ramspol, Literatuuronderzoek en rekenkundig onderzoek (Dutch), Delft Hydraulics

Meijer, D.G., januari 1993, Balgstuw Ramspol, verslag modelonderzoek, Q1545, Waterloopkundig Laboratorium.

Milgram, J.H. (1971) Forces and motions of a flexible floating barrier, Journal of Hydronautics, Vol. 5, Number 2, April 1971, pp 41 - 51

Modak, T.B., March 1967, Roll-up and fold-away dams, Journal Institution Engineers (India), 47, no.7, part C14, p.472-474.

Muramatsuu, T., "Auto Rubber Dam" in flood conditions, Dept. of Marine and Civil Engineering, Bridgestonde Tire Co. Ltd.

Nakamura Y. and T.Mizota (1971) Aerodynamic characteristics and flow patterns of a rectangular block, Report of Research Institute for Applied Mechanics, Kyushu University, 19(65).

Namias, V., December 1985, Load-supporting fluid-filled cylinderical membranes, Journal of Applied Mechanics, Vol.52, p.913-918.

Newman, J.N., 1994: Wave effects on deformable bodies, J. of Applied Ocean Research 16, pp.47-59.

Nickels, H. and G.Heerten, 1996: Building elements made of geosynthetics and sand resist the North Sea surf, Proc. of the 1st European Geosynthetic Conf. Eurogeo 1, Maastricht.

Nieuw type zinkstuk ontwikkeld voor kustvakken, rivieroevers en voor pipelines, article in OTAR, 11 pp 357 (1992),

Oberleitner, P. and Vischer, D., 1983, Schlauchwehre, Wasser, Energie, Luft, 75, no.4, p.95-97.

Ogihara, K., September 1983, Auto-rubber dam under flood conditions, Int. Conf. on the Hydraulic Aspects of Floods & Flood Control, London, Cranfield, BHRA, paper C4, p.99-108 ref.

Ogihara, K. and H. Saito, September 1984, Rubber dam, Proceedings Fourth congress Asian and Pacific Division of International Association of Hydraulic Research, Chiang Mai, Vol. I, pp 593-602

Ogiwara, K., Tateish, T. and Furuya, H., 1970, The shape of the rubber dam, Proceedings, Japan Society of Civil Engineering, Vol.179, No.7, p.37-47.

Ohyama, T., M.Tanaka, T.Kiyokawa, T.Uda, and Y.Murai, 1989: Transmission and reflection characteristics of waves over a submerged flexible mound, Coastal Engineering in Japan 32(1), pp.53-68.

Paolina, R. and Terziani, A. and Degrada, B., 1989, Example of a flexible weir built to replace needle weir (poiree) on the river Tanaro, Conference on Civil Works, Zürich.

Parbery, R.D., 1976, A continuous method of analysis for the inflatable dam, Proceedings of the Institution of Civil Engineers,, Vol. 61-part 2, p.725-736.

Parbery, R.D., September 1978, Factors affecting the membrane dam inflated by air pressure, Proc. Inst. Civ. Eng., Part 2, 65, p.645-654.

Pemič, A., 1976, Hydraulic model study of drop spillways on the Savinja river, (In Slovenian with English summary), Annual Digest of Research Work, Vodogradbeni Laboratorij v Ljubljana, p.29-32.

Plaut, R.H. and S. Suherman, 1997, Two-dimensional analysis of geo-synthetic tubes, submitted to Journal of Geotechnical en Geo-environmental Engineering, ASCE

Pover, J.P., June 1993, Berekening Balgstuw Ramspol (Dutch), Rijkswaterstaat

Pilarczyk, K.W., 1995, Novel systems in Coastal Engineering, geotextile systems and other methods, Rijkswaterstaat, Road and Hydraulic Engineering Division, Delft, The Netherlands.

Provinciale Waterstaat en Planologische Dienst van Zuid-Holland te Den Haag, 26 juli 1965, Beweegbare balgstuw of dergelijke waterkering, Octrooiraad-Nederland, aanvrage no. 6506682.

Rankilor, P.R., 1989, The reduction of soil erosion by preformed systems, The Intern. Erosion Control Association, Symp. on Soil Erosion and its Control.

Regeling, H.J., 1989, Balgstuw oriënterend onderzoek, verslag modelonderzoek, Q1025, Waterloopkundig Laboratorium.

Reiffsteck, P. and J.F.Vignon, 1996, Innovative, protective three dimensional geocomposite for bank protection: a case study, Proc. of the 1st European Geosynthetic Conf. Eurogeo 1, Maastricht.

Rijkswaterstaat, Bouwdienst, 1996, Opblaasbare kering Kampen.

Sawaragi,T., S.Aoki and A.Yasui, 1989, Tension on silt curtains in currents and waves, Eight International Conference on Offshore Mechanics and Arctic Engineering, The Hague 19-23 March pp 13 - 21

Sawaragi, T., S.I. Aoki, H. Liu, June 1992, Wave-induced impulsive forces in tension cables of a floating silt curtain, Proceedings of the Second International Offshore and Polar Engineering Conference, San Francisco, USA, Vol 3, No 2, 14-19, pp 339 -346

Sawaragi, T., 1995, Coastal engineering- waves, beaches, wave-structure interaction,Elsevier, pp 259 and further.

Schröder, W. and Sulser, P., July 1977, A new type of intake structure suitable for arid conditions, Erosion and solid matter transport in inland waters, Symposium, Paris, Washington, D.C., Int. Ass. Hydrol. Sciences, IAHS publ. no.122, p.338-343.

Seymour, R.J. and G.M.Hanes, 1979, Performance analysis of tethered float breakwater, ASCE, J. of waterways, Port, Coastal and Ocean Engineering, Vol.105(3), pp.265-281.

Sheperd, E.M., McKay, F.A. and Hodgens, V.T., Jan.-Febr. 1969, The fabridam extension on Koombool oomba dam of the Tully falls Hydro-electric power project, The journal of the Institution of Engineers, Australia, 41, no.1-2, p.1-7.

Sluis, C.M. et al, 1995, Bergbezinkzakken voor schoner oppervlaktewater, Stadswater, jaargang 24, pp.4-95.

Sollitt, C.K., C.P.Lee, W.G.McDougal and T.J.Perry, 1986, Mechanically coupled buoyant flaps: theory and experiment, Proc. 20th Coastal Engineering Conf., Vol.3, pp.2445-2459.

Sumitomo Electric, 1988, Sumigate-Inflatable rubber gate, Commercial Brochure.

Taiyo Kogyo Corporation, 1994, Design of Silt Protector, company publication, Tokyo, Japan.

Takasaki, M., November 1989, Omata inflatable weir, at the Kawarabi Hydro Scheme, Japan, Water Power and Dam Construction, Vol.41, no.11, p.39-41.

Thompson, G.O. C.K.Sollitt, W.G.McDougal and W.R.Bender, 1992, Flexible membrane wave barrier, Proc.Ocean V, ASCE, New York, pp.129-149.

Voskamp, W., 1983, Construction of steep slopes of sand under water using synthetic fiber screens, 2nd Intern.Offshore Mechanics and Arctic Engineering Symp., Houston, Texas.

Vries, J.T. de, 1988, Kunststofkeringen, Rijkswaterstaat, Hoofdafdeling Sluizenbouw, projectnr. 186700.

Wang, K.H. and X.Ren, 1993, Water waves on a flexible and porous breakwater, ASCE, J. of Engineering Mechanics 119, pp.1025-1048.

Watson, R., 1985, A note on the shape of flexible dams, Journal of hydraulic research, Vol. 23, no 2, 179 - 194

Wiegel, R.L. et al, August 1958, Model study of wind wave abetement, Institute of Engineering Research, Univ. of califormia, WRL Field report n0 49,

Williams, A.N., P.T.Geiger and W.G.McDougal, 1991, Flexible floating breakwater, ASCE, J. of waterways, Port, Coastal and Ocean Engineering, Vol.117(5), pp.429-450.

Williams, A.N., P.T.Geiger and W.G.McDougal, May 1992, A submerged compliant breakwater, J. Offshore Mechanics and Arctic Engineering Conf. 114, pp.83-90.

Yildiz, D., 1989, On scale models for inflatable weirs, IHE, Delft.

Zhao, R., 1994, Hydroelastic analysis of a floating flexible body in waves, Proc. 9th Intern. Workshop Water Waves and Floating Bodies, Kuju, Japan, pp.241-244.

WL | delft hydraulics

Rotterdamseweg 185
postbus 177
2600 MH Delft
telefoon 015 285 85 85
telefax 015 285 85 82
e-mail info@wldelft.nl
internet www.wldelft.nl

Rotterdamseweg 185
p.o. box 177
2600 MH Delft
The Netherlands
telephone +31 15 285 85 85
telefax +31 15 285 85 82
e-mail info@wldelft.nl
internet www.wldelft.nl